DESIGN AND DEVELOPMENT OF UPSCALED AUTOMATED PHASE CONTROLLED IMPACT DEVICE FOR OPERATIONAL MODAL TESTING

Universiti Malaya

LEE DERK HUAN

FACULTY OF ENGINEERING
UNIVERSITY OF MALAYA
KUALA LUMPUR

2019

DESIGN AND DEVELOPMENT OF UPSCALED AUTOMATED PHASE CONTROLLED IMPACT DEVICE FOR OPERATIONAL MODAL TESTING

LEE DERK HUAN

Universiti Malaya

THESIS SUBMITTED IN FULFILMENT OF THE REQUIREMENTS FOR THE DEGREE OF MASTER OF MECHANICAL ENGINEERING

FACULTY OF ENGINEERING
UNIVERSITY OF MALAYA
KUALA LUMPUR

2019

UNIVERSITY OF MALAYA

ORIGINAL LITERARY WORK DECLARATION

Name of Candidate: Lee Derk Huan Matric No: KQK 180004

Name of Degree: Master of Mechanical Engineering

Title of Project Paper/Research Report/Dissertation/Thesis ("this Work"):

Design Development of Upscaled Automated Phased Controlled Impact Device for Operational Modal Testing

Field of Study: Vibration

I do solemnly and sincerely declare that:

(1) I am the sole author/writer of this Work;
(2) This Work is original;
(3) Any use of any work in which copyright exists was done by way of fair dealing and for permitted purposes and any excerpt or extract from, or reference to or reproduction of any copyright work has been disclosed expressly and sufficiently and the title of the Work and its authorship have been acknowledged in this Work;
(4) I do not have any actual knowledge nor do I ought reasonably to know that the making of this work constitutes an infringement of any copyright work;
(5) I hereby assign all and every rights in the copyright to this Work to the University of Malaya ("UM"), who henceforth shall be owner of the copyright in this Work and that any reproduction or use in any form or by any means whatsoever is prohibited without the written consent of UM having been first had and obtained;
(6) I am fully aware that if in the course of making this Work I have infringed any copyright whether intentionally or otherwise, I may be subject to legal action or any other action as may be determined by UM.

Candidate's Signature Date:

Subscribed and solemnly declared before,

Witness's Signature Date:

Name:

Designation:

University of Malaya

ABSTRACT

In recent years, lab-scale Automated Phase Controlled Impact Device (APCID) for small rotating machines had been successfully developed for Impact-Synchronous Modal Analysis (ISMA). In response to this, an upscaled APCID is developed for medium sized industrial machines. The concept designs are first generated to meet the design requirements of creating a high impact force device that is supported by a safe, reliable, robust and portable base. A weighted selection matrix is used to evaluate the concepts to select the most suitable concept for design development. Solidworks is used to develop detail drawings in 2D and 3D for fabrication and computational analysis purpose. ANSYS Workbench 19.1 is used to perform static and dynamic analysis on the upscaled APCID design. The analysis showed that the selected APCID design is structurally safe and will not fail during operation as the safety factors are all more than 1. As such, a prototype weighing 32kg is fabricated and the overall dimension is 1390 x 420 x 1025 mm (L x W x H) and 700 x 420 x 820 mm (L x W x H) for fully extended and folded configurations respectively. The upscaled APCID is recalibrated using solenoid voltage level, activation time of solenoid and separation distance to ensure the device can supply high impact force to excite the industrial machines as well as generate smooth impact profiles that are similar to the lab-scale APCID. Generally, the impact force increases with increase of voltage level but increases until a limit and then decreases for increase in activation time of solenoid and separation distance. At 42V, the maximum impact force achieved is 259.702 N and 346.297 N for vertical and horizontal impacts. This is achieved using an activation time of 50ms for both cases and 7mm and 8mm separation distance for vertical and horizontal impacts respectively. In conclusion, the upscaled APCID developed is a success as it generates impact force as required to perform ISMA on industrial machines.

Keywords: ISMA, APCID, impact force, computational analysis.

Universiti Malaya

ABSTRAK

Kebelangkaan ini, Alat Pukulan Automatik yang Dikawal oleh Fasa (APCID) yang bersaiz kecil telah berjaya diperkenalkan untuk pengujian modal secara ISMA. Oleh itu, APCID yang berskala besar yang sesuai untuk pengujian ISMA ke atas mesin industri yang bersaiz sederhana akan direka dalam projek ini. Konsep reka bentuk yang mempunyai ciri-ciri daya impak yang tinggi akan digabungkan dengan reka bentuk tapak yang selamat dan kuat. Konsep-konsep yang dijana ini akan dinilai dengan menggunakan matrix pilihan untuk memilih reka bentuk yang paling bagus untuk diteruskan. Lukisan terperinci dalam 2D dan 3D akan dilukis dalam Solidworks untuk pengiraan analisa dan fabrikasi. ANSYS Workbench 19.1 pula digunakan untuk menganalisa konsep reka bentuk APCID tersebut secara static dan dinamik. Hasil kajian ini menunjukkan bahawa konsep reka bentuk APCID berskala besar adalah selamat dan tidak gagal kerana faktor keselamatannya melebihi 1 dalam kesemua analisa. Prototaip APCID yang berskala besar yang dibina berdasarkan reka bentuk tersebut mempunyai berat 32kg dan berukur 1390 x 420 x 1025 mm (P x L x T) and 700 x 420 x 820 mm (P x L x T) dalam konfigurasi terbuka dan tertutup. APCID berskala besar ini juga dikalibrasikan dengan menggunakan voltan, masa aktivasi dan jarak pemisahan antara solenoid dan permukaan impak untuk memastikan profil impak adalah berkeadaan baik seperti profil impak APCID berskala kecil. Pada 42V, daya impak maksimum sebanyak 259.702 N dan 346.297 N telah berjaya dikesan untuk pukulan secara menegak dan mendatar. Daya impak ini adalah dikesan dengan menetapkan masa aktivasi sebanyak 50ms untuk kedua-dua cara pukulan dan jarak pemisahan sebanyak 7mm dan 8mm untuk pukulan secara menegak dan mendatar. Sesungguhnya, APCID berskala besar telah berjaya dihasilkan kerana ia mampu menjana daya impak yang mencukupi untuk melaksanakan ujian ISMA ke atas mesin industri yang bersaiz sederhana.

Kata Kunci: ISMA, APCID, daya impak, analisa pengiraan.

ACKNOWLEDGEMENTS

I wish to take this chance to extend my express my appreciation to my supervisor, Ir. Dr. Ong Zhi Chao, for his insights and advices which guided me towards the completion of this research project. His knowledge and support given are invaluable in the research progress. I am very thankful for all the staff of University Malaya who have assisted in the completion of this research project. This research project would not have been possible without the advice and financial support given by Advanced Shock and Vibration Research Group of University Malaya. I am also taking this oppurtunity to thank my supportive family and friends for their motivation and encouragement. Last but not least, I would like to sincerely thank all my friends for their guidance and advices in assisting me towards the completion of this research project.

Universiti Malaya

TABLE OF CONTENTS

Universiti Malaya

Universiti Malaya

Universiti Malaya

Universiti Malaya

LIST OF FIGURES

Universiti Malaya

Universiti Malaya

LIST OF TABLES

Universiti Malaya

LIST OF SYMBOLS AND ABBREVIATIONS

APCID	:	Automated Phase Controlled Impact Device
EMA	:	Experimental Modal Analysis
OMA	:	Operational Modal Analysis
ISMA	:	Impact-Synchronous Modal Analysis
ISTA	:	Impact-Synchronous Time Averaging
FRF	:	Frequency Response Function
FFT	:	Fast Fourier Transform
AID	:	Automated Impact Device

Universiti Malaya

CHAPTER 1: INTRODUCTION

1.1 Introduction

In this chapter, background information regarding automated phase controlled impact device is presented. The mechanism and basic principles of the device are discussed in detail here. Furthermore, the significance and objectives of this research are established. Lastly, an outline for all five chapters of this research project report are briefly described.

1.2 Research Background

A rotating machinery often operates at high rotational speed to achieve high efficiency standards. Any inherent imbalance or defects in the rotating components will give rise to problems related to vibration during operation. When the vibration frequencies coincide with the natural frequency of the structure, the machine will resonate at unacceptably large amplitudes and eventually fail. Therefore, it is crucial to understand a machine's dynamic characteristics to predict its behavior under harmonic excitation.

Generally, the dynamic response of a structure is governed by three main parameters namely, modal frequency, damping and mode shapes (Thomson & Dahleh, 2013). Modal analysis is a common and established tool that is used in various engineering fields to determine these parameters. Engineers use the modal parameters for a wide range of applications such as design optimization, vibration control, structural health monitoring and damage detection (Cakir & Uysal, 2015; Collinger et al., 2009; Garcia-Perez et al., 2013; Xu et al., 2016).

Modal analysis testing typically involves 3 simple procedures. The displacement signal of a vibrating structure is first collected in the time domain with a sensor such as displacement sensor or accelerometer. Fast Fourier Transform (FRF) is then used to transform the time domain signal into the frequency domain. Finally, modal parameters are extracted to build a mathematical model of the structure for further evaluation.

Modal analysis has evolved over the past 40 years with various techniques which are categorized into two main groups, namely Experimental Modal Analysis (EMA) and Operational Modal Analysis (OMA). In EMA, the system is artificially excited with a measurable known input force and the output response data are measured in controlled environments. Hence, this technique would require the system to be in complete shutdown as any unaccounted external and internal dynamic forces will affect the results accuracy. These constraints limit the practicality of EMA on large complex structures such as petrochemical plants where downtimes are costly (Rahman et al., 2011b)

OMA is an output only modal analysis where the modal parameters are extracted without measuring the input force. This allows it to be more practical as the system does not need to be shut down for testing and the measured response is reflective of the real operating conditions. However, the modal parameters such as mode shapes cannot be normalized accurately for further analysis as the input excitation force is unknown.

A novel modal analysis technique known as Impact-Synchronous Modal Analysis (ISMA) was introduced in recent years to improve operational modal testing process (Lim et al., 2018a). ISMA artificially excites a system and measures its response similar to EMA but does not require the system to be shutdown. This technique integrates Impact-Synchronous Time Averaging (ISTA) to filter out asynchronous harmonic disturbances by averaging the signals collected for accurate modal parameter extraction.

ISMA possess the positive attributes of EMA and OMA and is considered as a hybrid of these two techniques. However, a high number of averages is required to do away with the disturbances when manual impacts are performed on structures with dominant cyclic loads (Rahman et al., 2011b). As the rate of impact of manual impact hammer is random and not synchronized with the disturbances, the effectiveness is reduced.

Universiti Malaya

Research done in the post processing stage had demonstrated that the number of averages can be reduced to increase the effectiveness of ISMA. This is achieved by controlling the phase angle between the vibration forces and the artificial excitation impact. This phase synchronisation effect is studied extensively under laboratory condition with an Automated Impact Device (AID) developed by Ong et al. (2015).

ISMA with phase selection assessment tested on small scale machines showed that less than 5 averages are enough to eliminate the asynchronous components. This allows for a faster modal identification through a straightforward way of eliminating the periodic response. This was achieved using a lab-scale Automated Phase Controlled Impact Device (APCID) which was capable of generating forces up to 100N only.

As industrial machines are subjected to higher excitation forces, the current APCID impact force is too low to be distinguishable for ISMA modal parameter extraction. For a medium sized machine, a larger impact force between 200N to 500N is required for the impacts to be distinguishable from the cyclic loads. Thus, the work is extended to real industry application as this research project focuses on the design development of an upscaled APCID suitable to perform ISMA on medium sized industrial machine.

1.3 Problem Statement

ISMA has been gaining popularity in recent years as it combines the benefits of EMA and OMA and is used for various applications. As the operating system cyclic response is filtered out using ISTA, the modal parameters of the system are extracted while the machine is in normal operation. As such, the system does not need to be shutdown for modal analysis using ISMA. Therefore, ISMA is the preferred technique in industries where machine downtimes are costly such as the oil and gas industry.

Universiti Malaya

ISMA studied under laboratory conditions have produced better modal identification results efficiently. For modal analysis to be performed on industrial machines, large impact forces are needed to excite the system. However, the impact force generated by the current lab-scale automated impact device of 100 N is insufficient for real life industrial machine applications. As medium sized industrial machines operate at 0 to 100 Hz, it would require an impact force ranging from 200N to 500N for modal parameter identification using ISMA.

In response to this problem, this research project intends to design and develop an upscaled APCID to test the phase synchronization effect on medium sized industrial machines. The upscaled APCID investigated aims to generate a larger impact of between 200N to 500N while supported by a sturdy and portable base. Computational analysis is also used to determine the structural integrity of the upscaled APCID design.

1.4 Objectives

The objectives of this research project are as follow:

1. To design an upscaled APCID with enlarged impact force
2. To evaluate the structural integrity of the upscaled APCID design through computational analysis
3. To fabricate a functional upscaled APCID design prototype
4. To recalibrate the upscaled APCID impact force level based on the optimum solenoid voltage level, solenoid activation time and separation distance.

Universiti Malaya

1.5 Scope

The scope of this research project is limited to designing of an upscaled APCID for medium sized industrial machine application. A medium sized industrial machine typically operates at a rotational speed between 0 Hz to 100 Hz with a 3-phase motor of 3 to 15 kW. The typical dimension of a medium sized industrial machine ranges between 800 x 300 x 500mm to 1200 x 600 x 800 mm (L x W x H). As such, the impact force required for a medium sized industrial machine ranges between 200 N to 500 N.

The APCID is designed to have rotatable solenoid to allow for multi axis impacting. In this research project, the APCID design will be analyzed for structural integrity when impact force is applied in the horizontal and vertical impact directions only. This is because these impacts are imparted at the extremities of the solenoid orientation and thus will result in the maximum possible response that the APCID will experience.

1.6 Thesis Outline

This research paper consists of 5 chapters and its contents are described briefly here. Chapter 1 introduces ISMA and APCID with a brief historical background of its developments to date. This is followed by the problem statement, objectives, scope and methodology of the research. Lastly, an outline of the report is listed down methodologically.

For Chapter 2, past researches and published results on ISMA, AID and APCID are reviewed and compiled in the literature review. This chapter aims to deepen the understanding on the working principles of ISMA and the control strategies of an APCID. Past results and developments on modal operational testing published by researchers are compressed into a concise summary for better understanding ISMA and APCID.

Universiti Malaya

In Chapter 3, the methodology of concept design, computational analysis and fabrication of APCID is described in detail. The process of conceptualizing and evaluating the APCID design is included in this section. The computational domain and pre-processing methods used is accounted for in this chapter. The selection of material and the fabrication process of APCID are also presented in detail

In Chapter 4, the results obtained based on the selected design are analyzed and discussed in detail. The equivalent stress, total deformation and safety factor of the APCID design is presented in this section. The fabricated prototype of the upscaled APCID is also in this section. The factors that favors a higher impact force with a good impact profile are concluded and the optimum settings are then finalized. The phase synchronization effects of the prototype's operational modal testing are presented and compared with conventional methods in terms of their accuracy and effectiveness.

Lastly in Chapter 5, a conclusion is drawn from the discussion of the simulated and experimental results. Based on the limitations observed in the current experiment, suggestions for future studies are recommended to address these shortcomings.

Universiti Malaya

CHAPTER 2: LITERATURE REVIEW

2.1 Introduction

In this chapter, similar researches on modal analysis conducted by past researchers are reviewed. This chapter aims to better understand the characteristics of ISMA to determine the design considerations of the APCID. This summary of past investigations helps to comprehend the limitations encountered in past studies to avoid them in this research.

2.2 Modal Analysis

Modal analysis is a study conducted to identify the dynamic characteristics of a system by determining the three modal parameters, namely modal frequency, damping and mode shapes (Thomson & Dahleh, 2013). In order to develop a mathematical model of the system's dynamic behavior, two frequently used modal analysis techniques are EMA and OMA. The method used to excite a system is the main difference of these two techniques.

EMA focuses on post processing the response of a system due to a known measurable input by cross correlating these measured inputs. Fast Fourier Transforms are used to convert the correlated functions from time domain to frequency domain to extract the three modal parameters. This requires the system to be artificially excited with a manual impact hammer in a complete shutdown mode in order to ensure system is not induced with any unaccounted excitation forces as shown in Figure 2.1.

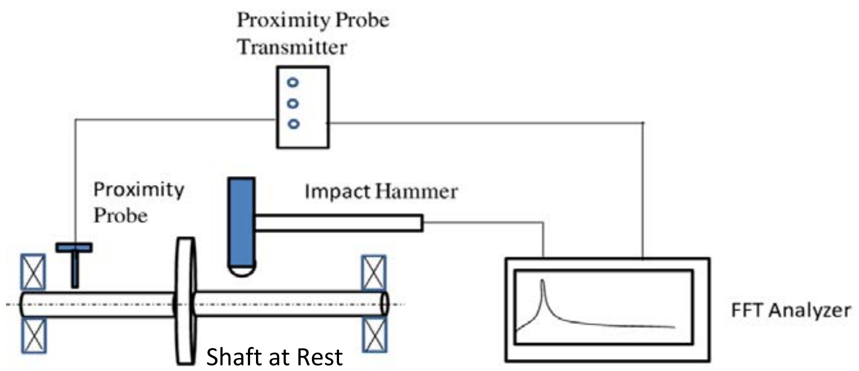

Figure 2.1: Typical setup of EMA testing with manual impact hammer

Universiti Malaya

OMA focuses on computing the three modal parameters based on only the response of a system due to its own operating forces. As the system's cyclic loads and ambient forces acts as the exciters, the system does not need to be excited manually with an impact hammer. Thus, the system can operate as usual with no downtime when this technique is applied as input excitation to the system is not measured. However, the main drawback of conventional OMA is its assumption of the operating force is broadband in spectrum but this is not true for system with predominantly cyclic loads (Mohanty & Rixen, 2004b).

Past studies have tried to improve OMA by looking into harmonic reduction using methods such as Stochastic Subspace-based Identification (SSI), Time-frequency Domain Decomposition (TFDD), Transmissibility Functions Based (TFB) (Joseph & Larbi, 2001; Le & Argoul, 2015; Maamar et al., 2019). Past researchers have also tried to improve the accuracy of OMA by developing modal identification algorithms. Qi et al. (2008) integrated OMA with harmonic wavelet filtering (HWF), correction technique of spectrum analysis (CTSA) and Hilbert transform (HT) for rotor systems. Mohanty and Rixen (2004a) used Ibrahim time domain algorithm to improve OMA is for systems that are excited with white stationary noise. However, the extracted mode shape parameter cannot be normalized accurately due to the lack of knowledge of the input forces applied.

2.3 Impact-Synchronous Modal Analysis (ISMA)

ISMA is proposed by Rahman et al. (2011a) to bridge the limitation of conventional OMA for applications of systems with predominantly cyclic loads. ISMA combines the advantages of EMA and OMA to improve the extraction of modal parameters. This technique focuses on digital signal processing of upstream data by integrating Impact-Synchronous Time Averaging (ISTA). Signal acquired from a vibrating system is processed using this time domain synchronous averaging technique to eliminate speed synchronous and random signatures.

Universiti Malaya

This allows the modal analysis testing to be carried out while the system is in operation. This technique has been applied successfully to determine the dynamic characteristics of structures without interfering with the normal operation of the system (Rahman et al., 2011b). However, Rahman reported that the application of ISMA is limited especially on large structures in which the impact force is relatively small compared to the operating cyclic loads. This is because the small impact forces are camouflaged by high operating cyclic loads causing it to be indistinguishable and filtered out by ISTA. Besides, random impacts made by conventional hammer would need a large number of impacts to find out the system dynamic characteristics (Rahman et al., 2013).

2.4 Factors Affecting Effectiveness of ISMA

The 4 main factors that govern the effectiveness of ISMA are number of impacts, impact force level, exponential windowing function, phase synchronization effect. Previous studies have shown that these factors assist in filtering out unwanted noise signatures in the measured data to improve the accuracy and effectiveness of ISMA.

2.4.1 Number of Impacts

In ISMA, the number of impacts applied on a structure increases the number of averages carried. With an adequate number of impacts, noise and unknown external excitations can be eliminated, leaving behind the impulse response only (Rahman et al., 2011a). This improves the accuracy of ISMA in identifying the modal parameters of the system when applied on an operating system.

Increasing the number of impacts is particularly effective when applied on structures under cyclic load and ambient excitations as demonstrated on a motor driven structure (Rahman et al., 2014). It was found that the number of impacts increases as the operating speed gets closer to the system's mode shape natural frequency as shown in Figure 2.2. This is because as the structure resonates, the dynamic response covers up the impulse thus requiring a higher number of impacts to be effective.

Universiti Malaya

(a)

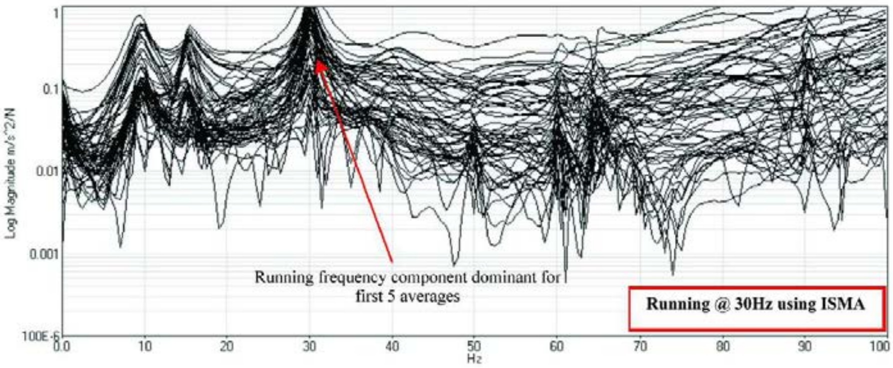

(b)

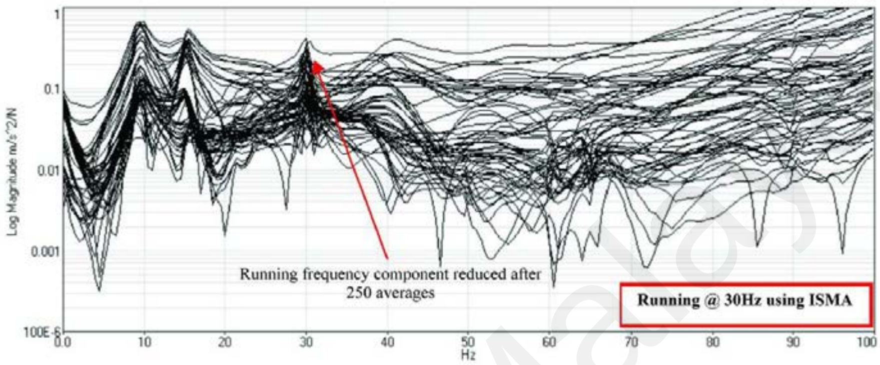

Figure 2.2: ISMA FRFs running at 30Hz with (a) 5 averages and (b) 250 averages (Rahman et al., 2014)

2.4.2 Impact Force Level

The impact force level is a very important factor to ensure the impulse response is distinguishable from the dynamic response. As the impact force increases, it is easier to excite the natural modes in the interested frequency range. However, excessive force may lead to non-linearity behavior of the structure resulting in a decrease in coherence of ISMA as demonstrated in previous study by Ong et al. (2016). The study shows that high impact force below the non-linearity force limit of the test rig are favorable to produce smoother Frequency Response Function (FRF) for modal parameters extraction.

2.4.3 Exponential Windowing Function

Signal attenuation and post processing method are also an important governing factor of ISMA performance. Exponential windowing function attenuates the amplitude of dynamic response signal to a small value exponentially as shown in Figure 2.3 making it suitable for modal testing performed under running conditions having harmonic loads.

Universiti Malaya

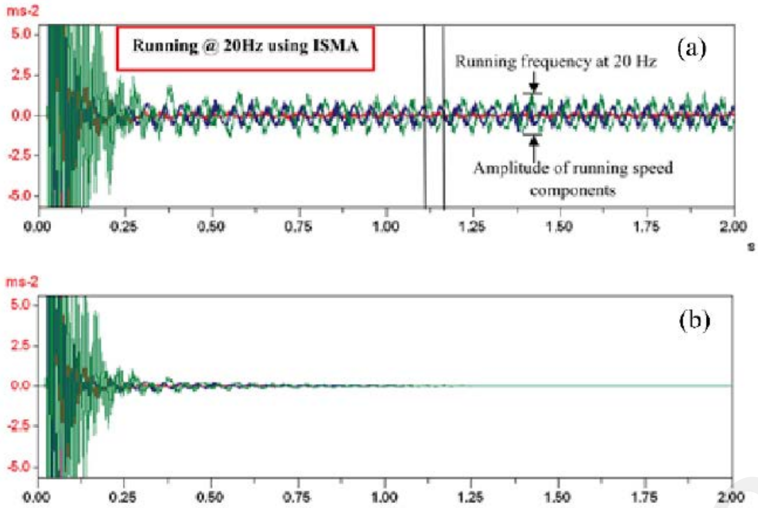

Figure 2.3: Acceleration time response at 20Hz for (a) no exponential window and (b) decay rate of 3 rad/s (Ong et al., 2016)

By averaging the response signals, exponential window function minimizes leakage of truncated response signal of low damped structures (Ong et al., 2016). It also eliminates the unaccounted forces responses in the time block to generate a better FRF of impulse response only. With a decay rate of 3 rad/s for the exponential windowing function, the accuracy of ISMA in extracting modal parameters is found to improve as the running frequency is diminished as shown in Figure 2.4.

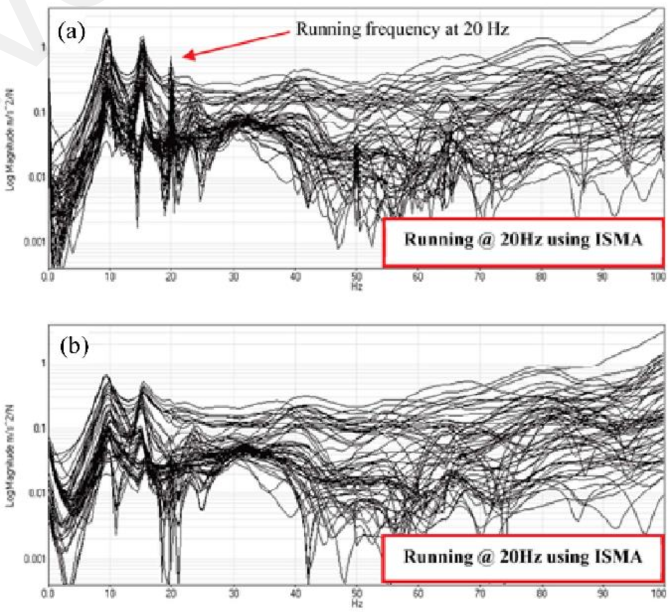

Figure 2.4: FRF estimation at 20 Hz for (a) no exponential window and (b) 3 rad/s) (Ong et al., 2016)

Universiti Malaya

2.4.4 Phase Synchronization Effect

Phase synchronization refers to synchronization of phase angles between the impact force and the periodic response of the operating system. When impacts applied are consistently in phase with the cyclic load response, non-synchronous excitation forces will appear with the same magnitude consistently and will not be averaged down by ISTA. However, when the impacts are applied at the out of phase with the cyclic load response, the non-synchronous excitation forces will be averaged down by ISTA.

Therefore, phase synchronization effect needs to be avoided in order to fasten the process of ISMA. It was found that the efficiency of ISMA can be improved significantly when the impact applied are not consistent with the phase angles and 180 degrees out of phase with the cyclic loads (Ong et al., 2017). This is because through averaging, the cyclic load components that are 180 degrees out of phase cancels each other out leaving behind the impulse response only.

In an ideal simulated scenario of inconsistent phase angles (Figure 2.5), only a minimum number of 4 impacts is required to eliminate all unaccounted forces for ISMA modal extraction (Ong et al., 2017). As manual impact hammers induce impacts at random and inconsistent phases, the improvement in effectiveness of ISMA is limited compared to the ideal case. In order to maximize the benefits of phase synchronization effects, a better control of the impacts applied is required to ensure the impacts at the correct phase and time.

Universiti Malaya

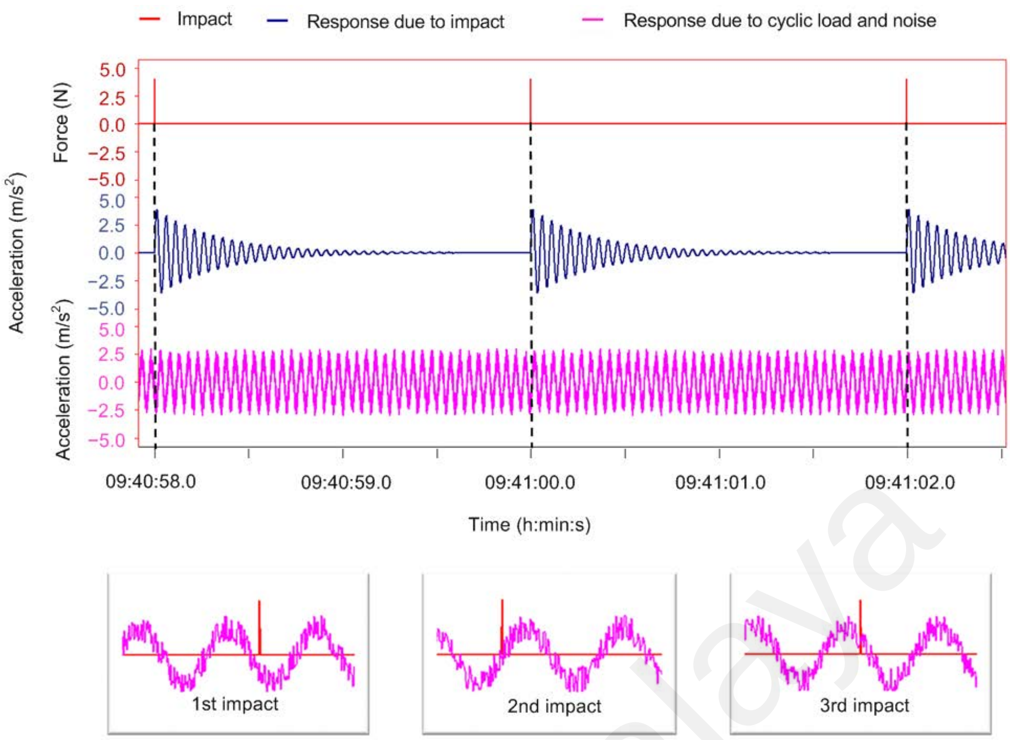

Figure 2.5: Impacts applied at inconsistent phase angles (Ong et al., 2017)

2.5 Automated Impact Device (AID)

Based on the factors that affects the effectiveness of ISMA, a portable calibrated AID is developed to bridge the gap of the past studies. The AID introduced by (Ong & Lee, 2015) imparts consistent non-synchronous impacts which are desirable for ISMA. The impact period, level and contact time of AID are determined in the literature to generate a good AID impact profile that are similar to impact profile of manual impact hammers as shown in Figure 2.6.

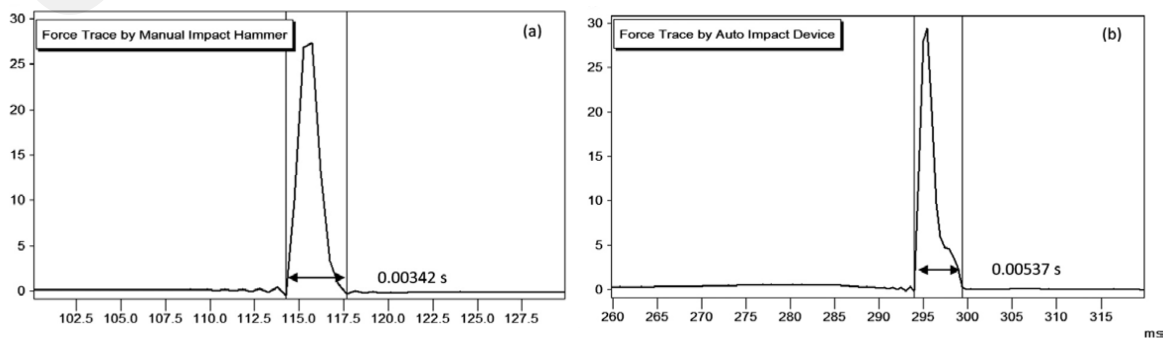

Figure 2.6: Comparison of impact profile of (a) manual impact hammer and (b) AID (Ong & Lee, 2015)

2.5.1 Components of AID

The AID developed consists of 3 main components, namely solenoid, sensors, data acquisition and control software. A solenoid is an electromagnetic coil winding that pushes and pulls a plunger housed within it. When supplied with a voltage, current passes through the coils inducing a linear electromagnetic force on the plunger. The stroke of this plunger imparts impact force on the test rig for modal analysis testing.

Accelerometers are used to pick up the displacement signal while force transducers measure the impact force made by the solenoid. These signals are sent to the data acquisition software for processing. LabVIEW software is used to control the energizing of the AID solenoid. By setting the time block and period of electric pulses, the activation time of the solenoid can be controlled to ensure consistent time interval between impacts.

2.5.2 Control of AID

The AID developed uses a digital square wave signal as the "on and "off" switch to impart non synchronous impacts at frequencies that are non-integer multiples of the harmonic response. Within the response block, the number of square waves, n is defined by Equation 2.1 where T is period of square wave t_{block} = Block Size / Sampling Rate.

$$n = \frac{t_{block}}{T} \tag{2.1}$$

The square waves will then progress when there is a time difference, $\Delta t = t_{block} - nT$.

The number of blocks of active pulses in the square wave, N is then evaluated with Equation 2.2 where t_{pulse} is the time for one active pulse in a period of square wave.

$$N = \frac{t_{pulse}}{\Delta t} \tag{2.2}$$

The solenoid on time, t_{on} is then expressed using Equation 2.3.

$$t_{on} = \left[\frac{t_{pulse}}{\Delta t}\right] \times t_{block} \tag{2.3}$$

Universiti Malaya

The impact interval is then calculated using Equation 2.4.

$$T_{impact} = \left[\frac{T}{\Delta t}\right] \times t_{block} \tag{2.4}$$

Finally, the frequency of the impact is calculated with Equation 2.5.

$$f_{impact} = \frac{1}{T_{impact}} \tag{2.5}$$

The AID impact force level is then calibrated by setting a voltage supply and energizing the solenoid until the point before the impact tip touches the surface to determine the optimum distance between the tip of the impact and the impact surface.

2.5.3 Advantages of AID

According to Ong and Lee (2015), it is noted that isolating the AID from the test rig as shown in Figure 2.7 improves the accuracy of the modal parameters extracted. The impact profile of this lab-scale AID is able to replicate the manual impact hammers for ISMA modal testing use. The results obtained using ISMA with this AID were comparable with results of EMA making it a suitable replacement of manual impact hammer. However, the timing of impact was not controlled making it unable to avoid the phase synchronization effect.

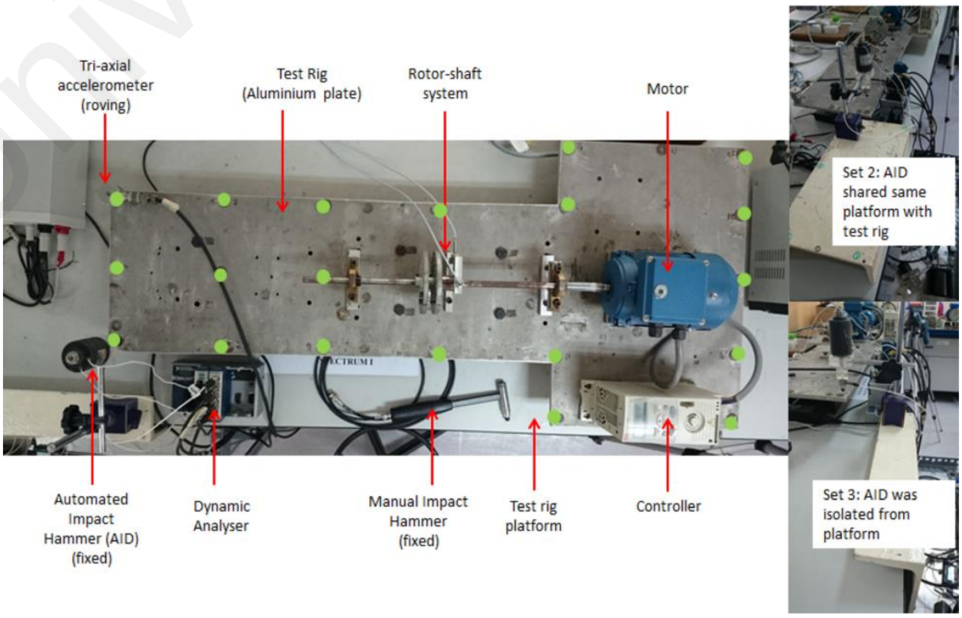

Figure 2.7: Setup of AID to investigate isolation effect (Ong & Lee, 2015)

Universiti Malaya

2.6 Automated Phase Controlled Impact Device (APCID)

Controlling of the timing of impact was introduced to AID to develop an APCID. Previous research has proven that 10 averages are adequate to filter out the asynchronous components. The effectiveness of ISTA improved with cleaner FRF and appearance of adjacent natural modes near operating speed as shown in Figure 2.8 (Lim & Ong, 2016). This presents an advantage over manual impact hammer as modal testing by ISMA faster.

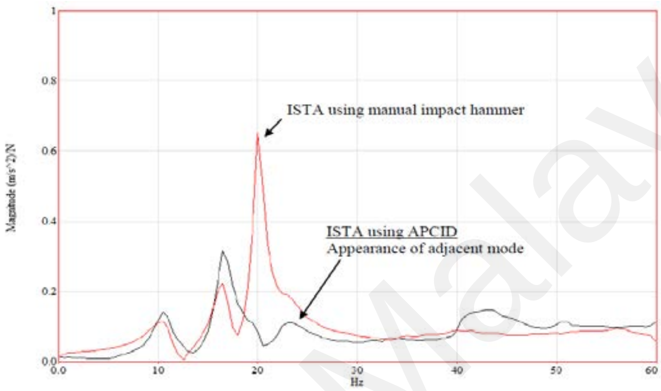

Figure 2.8: FRF comparison of ISTA using manual impact hammer and APCID (Lim & Ong, 2016)

2.7 Control Strategies of APCID

An initiation signal to detect the phase difference by utilizing a tachometer pulse signal to compare with the accelerometer was introduced to provide better control of the impact timing (Lim et al., 2018a). During operation, the signal of both tachometer and accelerometer give the same frequency with a constant time difference. Using cross power spectrum, phase difference between tachometer speed and dynamic response is obtained.

In general, the control system of an APCID consist of 2 stages, namely triggering and feedforward control of the impact device. In triggering stage, ample time delay, known as triggering time, T_{trig} ranging between 2 to 12 s needs to be taken into consideration. This is to allow time for data acquisition and ensure the test structure is restored to its initial condition after every impact. T_{trig} is calculated by using Equation 2.6 where n is number of time block length, BS is block size and SR is sampling rate.

Universiti Malaya

$$T_{trig} = n \times \frac{BS}{SR} \quad (2.6)$$

The control of the APCID utilizes the feedforward method illustrated in Figure 2.9. In this feedforward stage, the moment of impact, L_{real}, is kept as close as possible to the impact set point, L_{exp}. The set point depends on the desired impact moment such as the crest or trough of the cyclic response $T_{counter}$ is the moment in time an excitation signal is sent to the DAQ to initiate the impact.

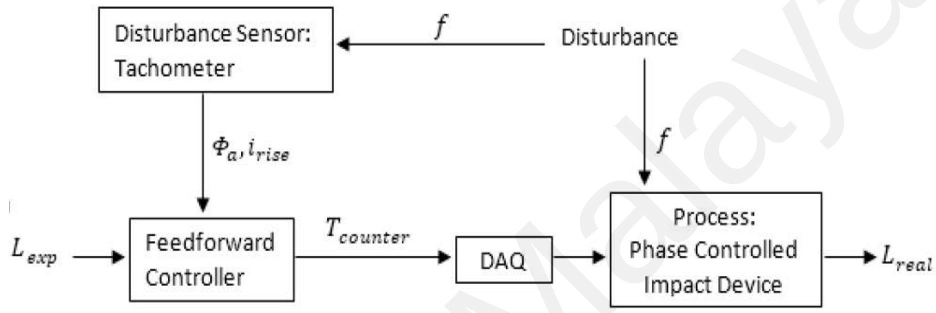

Figure 2.9: APCID feedforward control diagram (Lim et al., 2018a)

In an APCID, the operating frequency, f, phase difference, Φ_a and array index of rising edge, i_{rise} are parameters used to the control the impact device. Using this information, the phase difference time, T_Φ, load cycle time interval, T_{cycle}, time interval of desired impact, $T_{desired}$, and lag time, T_{lag}, is calculated by Equations 2.7 to 2.11. The lag time refers to the time interval between the last rising edge of the tachometer speed and the end of time block right after the impact is triggered.

$$T_{trig} = n \times \frac{BS}{SR} \quad (2.7)$$

$$T_\Phi = \left[-\frac{\Phi_a}{360°}\right] \times \frac{1}{f} \quad (2.8)$$

$$T_{cycle} = n \times \frac{1}{f} \quad (2.9)$$

$$T_{desired} = \left[-\frac{\Phi_p}{360°}\right] \times \frac{1}{f} \quad (2.10)$$

$$T_{lag} = [S_{ext} + S_{comp} - i_{rise}] \times \frac{1}{SR} \quad (2.11)$$

where S_{ext} is extracted samples from end of time block, S_{comp} is compensated sample.

Universiti Malaya

Another time delay to be considered is the offset time, T_{offset} due to the time difference between sending of the excitation signal to the time of real impact. This is determined through dummy impacts and is calculated using Equation 2.12.

$$T_{offset} = t_{real} - t_{exp} \tag{2.12}$$

where t_{real} is the moment of impact is observed in response signal and t_{exp} is the impact time before offset adjustment. Taking all these delay time into consideration, the final counter time, $T_{counter}$ sent to the DAQ to initiate an excitation signal to the APCID to impart and impact is calculated by Equation 2.13.

$$T_{counter} = T_{\Phi} + T_{cycle} + T_{desired} - T_{lag} - T_{offset} \tag{2.13}$$

The APCID uses this phase angle information to accurately trigger impacts at the correct timing to be always non-synchronous with respect to cyclic load response phase.

Although the APCID is able to control the timing of impact, the addition of tachometer limits the application to machine with exposed rotating parts only. In recent works by Lim et al.(2018b), the APCID is enhanced by using a tri-axial accelerometer to replace the tachometer for phase angle detection. This method focuses on using the filtered cyclic load response as the initiation signal in lieu of the tachometer pulse signal.

However, as the vibration response signal is tainted with noise and resulting in inaccuracies of the counter time. Therefore, band pass filter is used to filter out random noise making the peak of the response to be easily determined. As such the actual counter time must take into consideration the phase difference based on the filtered response and is determined using Equation 2.14.

$$T_{counter\_filter} = T_{\Phi\_\mathrm{filter}} + T_{cycle} + T_{desired} - T_{lag} - T_{offset} \tag{2.14}$$

This method not only addresses limitation of tachometer but also reduces the cost of APCID for modal analysis testing. The extracted modal parameters were found to be

Universiti Malaya

similar to the tachometer results making it a suitable replacement of the tachometer. Although the concept of APCID have been successfully demonstrated, the impact device is a small lab-scale solenoid that is able to impart impacts of up to 100 N only. Therefore, this research project purpose is to fill this gap by developing an upscaled APCID.

2.8 Summary

From this literature review, ISMA is a novel technique which merges the advantage of both classical EMA and OMA. ISMA has been developing rapidly in the past decade for operational modal analysis testing. The accuracy and effectiveness of ISMA are governed by four main factors, namely number of impacts, impact force level, exponential windowing function and phase synchronization effect. These factors are comprehensively studied in previous studies and are summarized in Table 2.1.

Table 2.1: Summary of factors governing effectiveness of ISMA

Governing Factors	Findings	Reference
Number of Impacts	• Sufficient number of impacts required to cancel out noise • High number of impacts required when operating speed is close to natural frequency	Rahman et al. (2014)
Impact Force Level	• High impact force excites the natural mode better while low impact forces may not be adequate to excite the vibrating machine • Force should not exceed the non-linearity limit for accurate results	Ong et al. (2016)
Exponential Windowing Function	• Exponential window minimizes leakages and eliminates unaccounted forces response • Decay rate of exponential window improves accuracy of ISMA	Ong et al. (2016)
Phase Synchronization Effect	• Minimum number of impacts required when impacts are made to be always out of phase with dynamic response	Ong et al. (2017)

Universiti Malaya

By introducing an AID, impacts can be imparted at fixed intervals with a consistent force level to improve the effectiveness of ISMA. The AID is found to be a good replacement of manual impact hammers as it produces a similar good impact profile. By further enhancing the APCID with a tachometer for phase angle detection, the timing of impacts can be controlled to avoid phase synchronization effects. This significantly reduces the number of impacts required for modal parameter extraction and increases the efficiency of ISMA. The APCID is further enhanced by replacing the tachometer with a tri-axial accelerometer which makes the impact more practical and less costly.

However, the enhanced APCID shown in Figure 2.10 is a lab-scale impact device that generate impacts of up to 100 N only. This impact force is insufficient for real life application where larger machines in operation have a larger dominant cyclic load force. In order to address the limitation of the enhanced APCID, this research project aims to develop a portable upscaled APCID that is effective, precise, robust and reliable for ISMA testing of medium sized rotating systems.

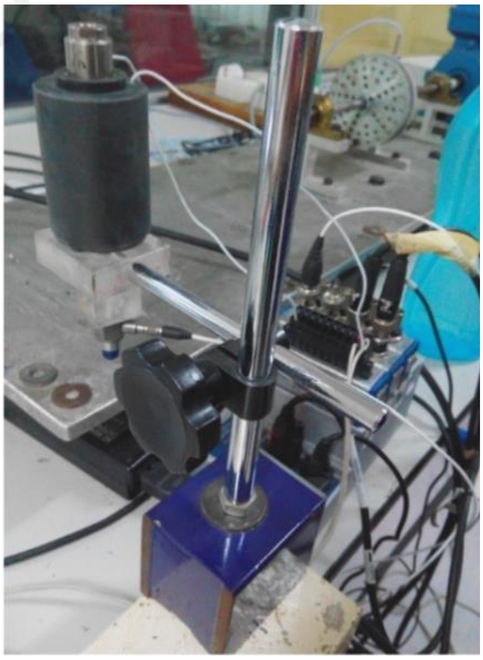

Figure 2.10: Previously developed lab-scale enhanced APCID (Lim & Ong, 2016)

Universiti Malaya

CHAPTER 3: METHODOLOGY

3.1 Introduction

The approach and methodology carried out to complete this research project is discussed in this chapter. Three different phases are used in this research project, namely conceptualization phase, design development phase and implementation phase. Design concepts of the APCID are first brainstormed according the design objectives. Computational analysis is then conducted using a combination of 3D modelling and simulation software. The fabrication methods and instrumentation used to test APCID prototype design are also discussed in this chapter.

3.2 Flow Chart

The overall flow of the project consists of 5 main activities and is illustrated using a flow chart as shown in Figure 3.1.

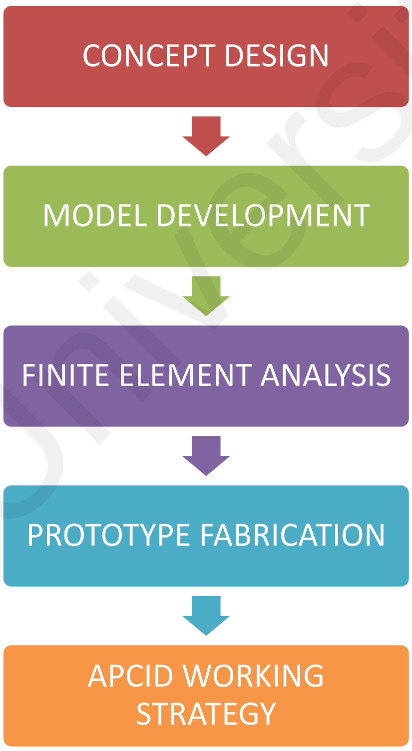

- Identify design requirement, concept generation and selection
- 3D modeling of concept design of upscaled APCID assembly and parts
- Perform static, dynamic, modal, harmonic response analyses using ANSYS
- Material procurement and prototype fabrication of finalized design
- Study on working and control strategy of upscaled APCID

Figure 3.1: Project flow chart

Universiti Malaya

3.3 Conceptualization Phase

In this phase, the concept design of an upscaled APCID is initiated by three activities, namely customer needs identification, concept generation and concept selection.

3.3.1 Customer Needs Identification

In this research project, the requirement of an APCID user are determined. Identifying the customer needs is a vital step in conceptualization phase in order to generate design ideas that serves the purpose of an APCID and satisfy the needs of the customers. A list of design requirement is compiled, and a weightage is assigned to each criterion according to its relative importance with a scale of 1 to 5 with 5 being the most desirable feature and 1 being the least desirable feature.

3.3.2 Concept Generation

In this activity, the identified needs of an upscaled APCID are transformed into conceptual designs. Design from previous research works are referred to during this brainstorming process in order to ensure the designs are feasible and practical. The advantages and disadvantages of each concept are then identified and improved until it is a fully developed concept.

3.3.3 Concept Selection

The fully developed concepts are then evaluated using a weighted selection matrix. The concepts are rated based on a scale of 1 to 5 on how well it satisfies the customer need with 5 being most satisfactory and 1 being least satisfactory. Each design criterion is weighted based on its relative importance and the total weighted score is tabulated. The concepts are then ranked according to their total weighted score and the highest ranking concept is chosen as the design of the upscaled APCID for this research project.

Universiti Malaya

3.4 Design Development Phase

In this phase, the selected concept is developed with detailed 2D and 3D drawings of the upscaled APCID design. The 3D model developed is then analyzed for its static and dynamic integrity using computational analysis software. The mathematical model used, meshing, boundary conditions and assumptions made are justified in this section. The estimated cost and procurement of material is also included in this chapter.

3.4.1 Detail Design

The concept design selected is developed into a detailed design complete with dimension and bill of material. Solidworks is used as the 3D modelling software to create detailed 2D and 3D drawings for fabrication purpose. Solidworks is selected as it is a common engineering modelling tool that is compatible with most computational analysis software such as ANSYS. In this process, suitable materials are also selected for each component in this process and its properties assigned in the 3D model. The materials used and its properties are tabulated in Table 3.1.

Table 3.1: Material properties of aluminium alloy and structural steel

	Aluminium Alloy	Structural Steel
Density (kg/m^3)	2770	7850
Poisson Ratio	0.33	0.30
Young Modulus (Pa)	7.10×10^{10}	20.0×10^{10}
Shear Modulus (Pa)	2.67×10^{10}	7.69×10^{10}
Tensile Yield Strength (Pa)	2.80×10^{8}	2.50×10^{8}
Compressive Yield Strength (Pa)	2.80×10^{8}	2.50×10^{8}
Tensile Ultimate Strength (Pa)	3.10×10^{8}	4.60×10^{8}

Universiti Malaya

3.4.2 Computational Analysis

Computational analysis is an iterative numerical investigation used to solve mathematical model for an approximate solution. In order to analyze the APCID's structural integrity, the 3D model created in Solidworks is exported into ANSYS Workbench 19.1 for static, dynamic, modal and harmonic response analyses using finite element method.

A typical finite element computational analysis involves three different processes, namely pre-processing, solving and post processing. In pre-processing, the geometry of the computational domain of Concept 1 is first defined using Solidworks. The 3D model is then exported into ANSYS for meshing into discrete finite elements of similar size. The boundary condition settings are also done in this pre-processing step to fully define the computational domain.

ANSYS Workbench 19.1 is used as the solver to investigate the structural integrity of the APCID. The finite element method is used to solve the governing partial differential equations of each discretized but connected elements. The stiffness matrices of each element are first calculated and then assembled into a global stiffness matrix for solving. The solution obtained is an approximate solution that is solved iteratively until an acceptable deviation is achieved. For structural integrity investigations, the stress, strain and deformation information are determined.

The post processing stage is the final stage of the computational analysis Using the post processor integrated in ANSYS software, results are plotted into graphical displays once the iterations are completed. The computational software transforms the output results into easy to analyze graphical forms such as contour plot, vector plot and surface plot depending on the user needs.

A graphical user interface is used in ANSYS to simplify the transformation process. As structural integrity is the main focus of the research, the safety factor of maximum stress under static and dynamic loads are extracted. The graphical results would then provide better insights and knowledge to help optimize the design.

3.4.3 Computational Domain and Meshing

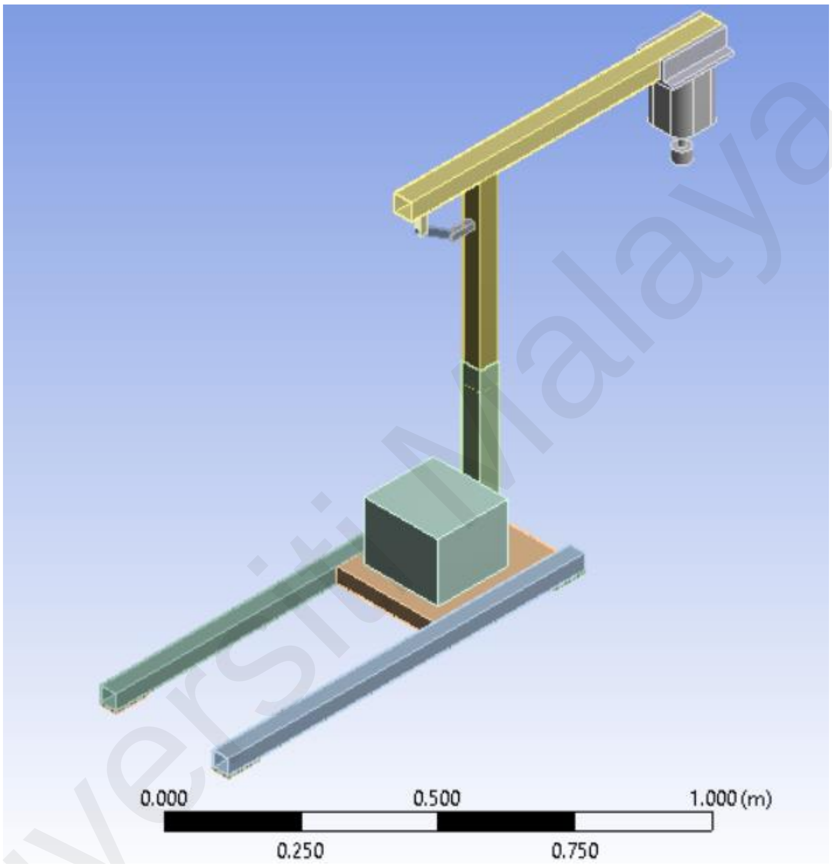

Figure 3.2: Simplified APCID design computational domain

The computational domain is the entire assembly of the APCID design concept as shown in Figure 3.2. The model is exported into ANSYS Workbench 19.1 for further pre-processing. The model used is a simplified version of the assembly to reduce the complexity of the system in order to speed up the solving process. Meshing is then carried out to discretize the entire assembly into discrete finite elements for solving.

Universiti Malaya

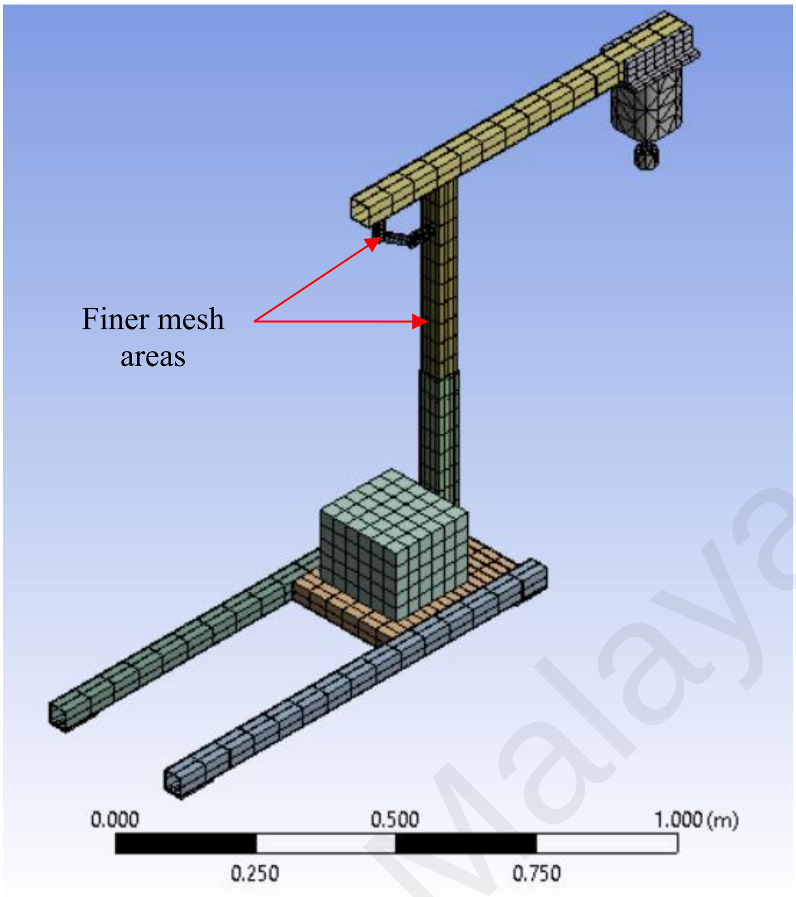

Figure 3.3: Quadrilateral dominant meshing of APCID design

An adaptive meshing method that is quadrilateral dominant is used as shown in Figure 3.3. A total of 2571 discrete elements with 12450 nodes each whereby each element has an average surface area of 0.012732 m^2 is obtained from the meshing. A high number of grid meshes are concentrated at critical areas such as the main supporting stem and the connecting links between the beam and supporting stem. This improves the accuracy of the simulation results of these components while shortening the computation time as larger grid sizes are located at less critical parts of the assembly.

Universiti Malaya

3.4.4 Boundary Conditions

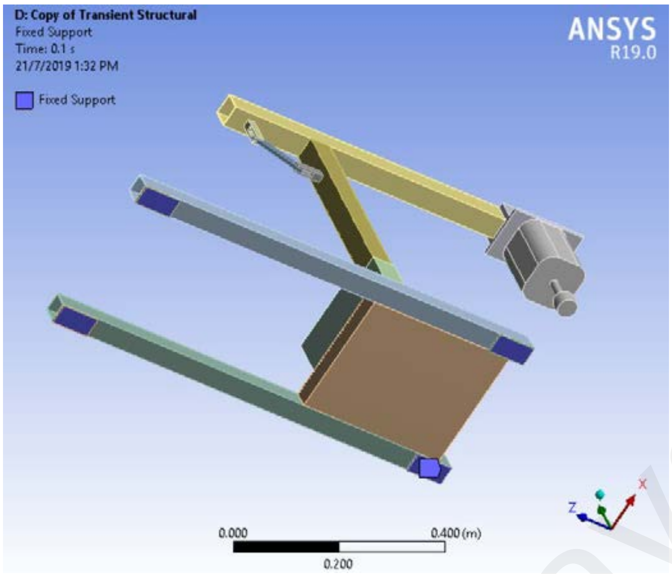

Figure 3.4: Location of fixed support boundary conditions

The boundary conditions used in the computational domain are fixed support and impact force boundary conditions. The fixed support boundary conditions are represented by the contact area between the casters and the floor as shown in Figure 3.4. For dynamic analysis, an impact force of 800N is included on the contact surface between the solenoid's acrylic with the machine as shown in Figure 3.5.

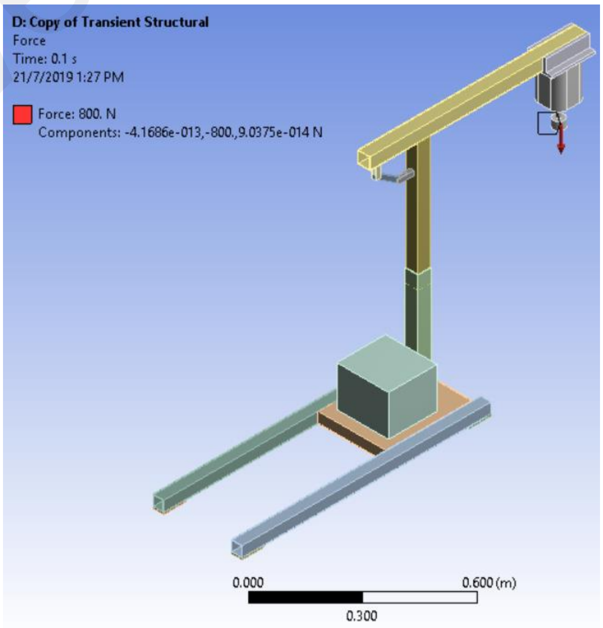

Figure 3.5: Location of impact force boundary condition

Universiti Malaya

3.4.5 Mathematical Models

The mathematical models used for computational modal analysis and failure analysis are presented in the following sections.

3.4.5.1 Modal Analysis

Modal analysis is used to determine the mode shapes of a vibrating structure and its corresponding natural frequencies. Frequencies and mode shapes of undamped systems are evaluated using Equation 3.1.

$$M\ddot{X} + KX = 0 \tag{3.1}$$

where M is the mass matrix and K is the stiffness matrix. Assuming the displacement X changes harmonically with time, Equations 3.2 to 3.4 are obtained.

$$X(t) = \bar{X}\sin(\omega t) \tag{3.2}$$

$$\dot{X}(t) = \omega\bar{X}\cos(\omega t) \tag{3.3}$$

$$\ddot{X}(t) = -\omega^2\bar{X}\sin(\omega t) \tag{3.4}$$

where $X, \dot{X}$ and $\ddot{X}$ are displacement, velocity and acceleration and $\bar{X}$ is the amplitude of nodal displacement vector. By substituting these into Equation 3.1, the Eigenvalue Problem (EVP) in Equation 3.5 is formed.

$$[K - {\omega_i}^2 M]\overline{X_m} = 0 \tag{3.5}$$

where eigenvalues $\omega_i (i = 1, 2, \dots, n)$ are the structure's natural frequencies and $\overline{X_m} (m = 1, 2, \dots, n)$ are the mode shapes.

3.4.5.2 Harmonic Response Analysis

The governing equation of a motion under damped forced vibration is defined in Equation 3.6 where $Q = F\sin(\omega t)$ is the harmonic loadings.

$$M\ddot{X} + C\dot{X} + KX = Q \tag{3.6}$$

Universiti Malaya

The equation is then transformed into its principal coordinates using Equation 3.7.

$$M_p\ddot{X_p} + C_p\dot{X_p} + K_pX_p = Q_p \tag{3.7}$$

where $Q_p = \emptyset^T Q$. The damped response to periodic excitation is given in Equation 3.8

$$\ddot{X_{pr}} + 2\sigma_r\dot{X_{pr}} + \omega_{or}{}^2X_{pr} = q_{pr}\sin\omega t \tag{3.8}$$

When solved, the magnitude and phase is calculated with Equation 3.9

$$X_{pr} = q_{pr}\beta_r\sin(\omega t - \theta_r) \tag{3.9}$$

where $\beta_r = \frac{1}{\sqrt{(\omega_{or}{}^2-\omega^2)^2+(2\sigma_r\omega)^2}}$ and $\theta_r = \frac{2\sigma_r\omega}{\omega_{or}{}^2-\omega^2}$. When transformed back into the original coordinated, Equation 3.10 is obtained for the harmonic response.

$$X = \sum_{r=1}^{n}\emptyset_rX_{pr} \tag{3.10}$$

3.4.5.3 Failure Analysis

The maximum equivalent von Mises stress is used as the effective stress value for the failure analysis. This is because the von Misses stress is an equivalent stress for the entire state of stress in a stress element and is derived in Equation 3.11 where σ_1 and σ_2 are the maximum and minimum principal stresses respectively.

$$\bar{\sigma} = \frac{1}{\sqrt{2}}[(\sigma_1-\sigma_2)^2 + (\sigma_2-\sigma_3)^2 + (\sigma_3-\sigma_1)^2]^{\frac{1}{2}} \tag{3.11}$$

The von Mises stress must always be lower than the yield stress to prevent any elastic deformation in the structural design.

Safety factor is a ratio of stresses used to check the structural integrity of a design. For static failure analysis, it is calculated using the maximum equivalent stress failure theory and failure is defined by yielding. The theory states that failure occurs when the maximum equivalent stress in a structure exceeds the yield strength of a material. Therefore, static safety factor calculated using Equation 3.12 must be greater than 1 to prevent any failure.

$$Static\ safety\ factor, \qquad n = \frac{\sigma_{eq}}{S_y} \tag{3.12}$$

Universiti Malaya

For fatigue failure analysis, the modified Goodman theory used is shown in Equation 3.13 and failure is defined by endurance limit, S_e. The endurance limit is the maximum value of cyclic stress a material can be applied without yielding. In this research, the design is checked for high cycle fatigue whereby the number of design cycles is 1,000,000 cycles. As the load applied is a fully reversed load, the mean stress, σ_m is zero and fatigue safety factor is expressed as shown in Equation 3.14.

$$Modified\ Goodman\ Theory, \qquad \frac{\sigma_a}{S_e} + \frac{\sigma_m}{S_{ut}} = \frac{1}{n} \tag{3.13}$$

$$Fatigue\ safety\ factor, \qquad n = \frac{S_e}{\sigma_a} \tag{3.14}$$

3.4.6 Assumptions

The 800 N force used in the dynamic analysis is assumed to be applied for 10 ms only to simulate an impact force. This impact force is higher than the designed maximum force of 500 N to compensate for the simplifications made to the design. This increases the safety factor of the assembled prototype by approximately twice of the computed results.

For both static and dynamic analysis, standard gravitational acceleration of 9.8066 m/s^2 acting vertically downward is applied to take the effect of the design's weight. All connections of surfaces in contact in the computational domain are assumed to be of bonded type. This is to ensure all connections simulated are rigid whereby no sliding or separation is allowed.

3.5 Implementation Phase

In this phase, a prototype is of the upscaled APCID is assembled based on the finalized optimized design. Based on the bill of material generated, a cost estimate is first prepared for budgeting purpose. The prototype is then fabricated according to the design once the materials are procured. Finally, the experimental setup to investigate the working strategy of the upscaled APCID is also included in this chapter.

Universiti Malaya

3.5.1 Cost Estimation

Cost estimation is used to draw up a budget cost for fabricating the APCID. The bill of material developed is used as a guide of materials to be procured. For standard parts such as aluminium profiles, connection joint, hinges and casters, the standard cost of these components are used. For custom components such as the solenoid, quotations are solicited from suppliers in order to estimate the cost of procurement. The budget of the project is then obtained by summing up all the material and manufacturing costs incurred.

3.5.2 Fabrication of APCID

Upon procurement of the raw materials, the upscaled APCID is assembled according to the detailed design drawings. The aluminium profiles are cut into the desired lengths and connected with joints, bolts and nuts. Holes are drilled and tapped as required to make way for the bolts and nuts. Safety precautions are taken during drilling and cutting by equipping oneself with personal protective equipment such as goggles and gloves to prevent any unfortunate events.

3.5.3 Measurement Procedure and Instrumentations

LabVIEW is used as to control the energizing of the solenoid using the response signal of the tri-axial accelerometer. The control system of the solenoid in this upscaled APCID used is similar to the control system configurations developed by Lim et al. (2018b)as discussed in Section 2.7. This ensures the solenoid can be controlled to impart timing when and where it is required. The list of instruments used are as follow.

1. Geeplus 874F Solenoid
2. ICP Force Sensor of Model No. 208C05 of measurement range up to 22.24 kN
3. NI USB Dynamic Signal Acquisition Module, Model NO-USB 9234
4. LabVIEW version 13.0
5. Powerflex Variable DC power supply, Model QPX1200S

Universiti Malaya

3.6 Experimental Setup

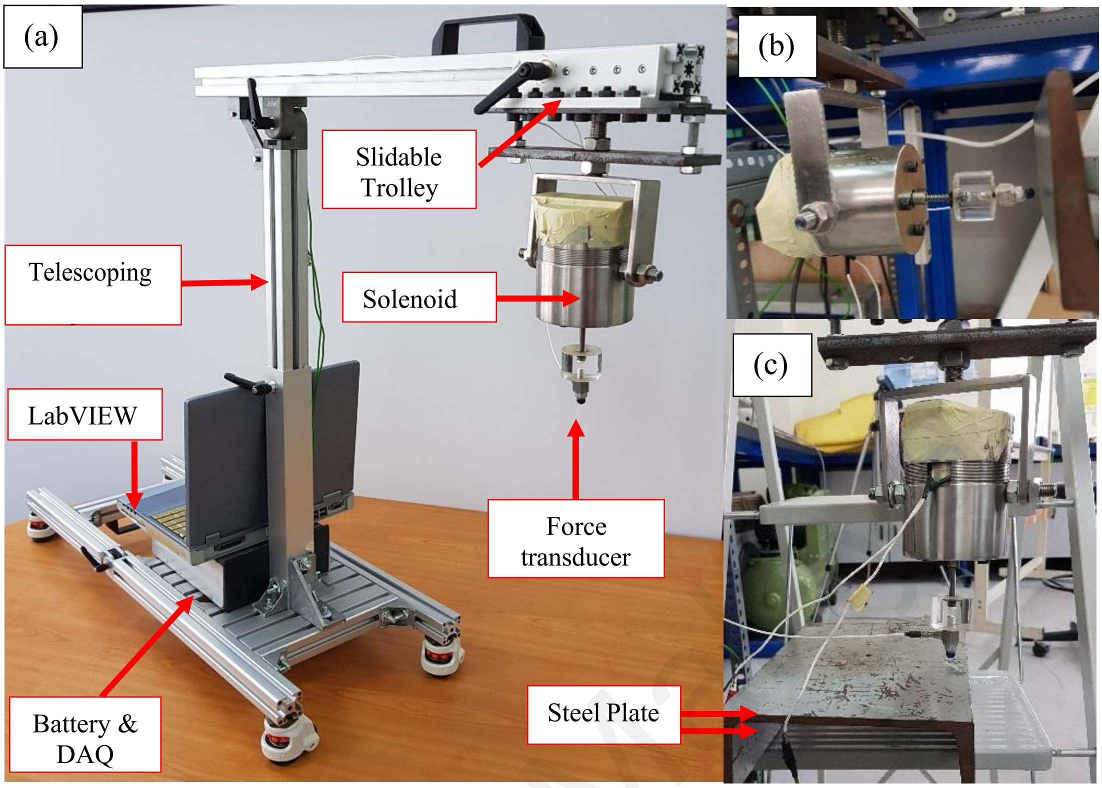

Figure 3.6: Experimental setup for impact force study. (a) Components of upscaled APCID, (b) horizontal impact setup and (c) vertical impact setup

In order to recalibrate the upscaled APCID, the experiment is setup as shown in Figure 3.6. The plunger impacts a flat steel surface in both horizontal and vertical directions is used as the impact surface and a force transducer located on the acrylic tip is used to measure the impact force and profile. The signals are sent to the data acquisition system at a sampling rate and block size of 2048 and 4096 samples respectively and sent to LabVIEW for further processing

For voltage level study, the voltage supplied to the solenoid is varied using a variable DC voltage power supply from 26 V to 44 V. For activation time study, the duration of time of the solenoid is varied between 50 ms to 65 ms by controlling its settings in LabVIEW. The separation distance is controlled by adjusting the height of the solenoid to vary between 5mm to 8mm. A total number of 5 impacts is performed and the average value is recorded and the smoothness of the impact profile is recorded.

3.7 Summary

In this chapter, the methodologies used from concept generation to design development and finally implementation are discussed. Concepts designs are first developed based on customer needs and then selected using a weighted selection matrix. A 3D model of the finalized concept is then modelled using Solidworks and the structural integrity of the concept is analyzed using ANSYS Workbench 19.1. The setup of the computational analysis and the pre-processing methods employed are described. Finally, the fabrication process of the upscaled APCID prototype is presented and the experimental setup used to determine its working strategies are also included.

Universiti Malaya

CHAPTER 4: RESULTS AND DISCUSSION

4.1 Introduction

APCID design concepts are generated and evaluation results in this chapter. The computational analysis results obtained are presented and discussed to evaluate the safety, reliability and robustness of the design. The upscaled APCID is subsequently recalibrated and the result is discussed in detail to determine the optimum settings of the design.

4.2 Conceptualization Phase

In this phase, the design requirements are first identified based on APCID user needs prior to generating concept designs. Three different concepts are then generated in this phase with features to satisfy the customer needs. These concepts are evaluated with a selection matrix and the most suitable concept is selected as the finalized concept design

4.2.1 Customer Needs Identification

The impact force level imparted by the APCID needs to be higher than the operating cyclic load for ISMA to be effective as demonstrated by Ong et al. (2016). For the lab-scale test rig used, the cyclic force experienced increased from 5N to 30N when the running frequency was increased from 20 to 30 Hz. As the medium sized industrial machine will operate at a higher frequency, a higher impact force would be required.

Based on the input from the industrial partner and past experience from the research team, a high impact force between 200N to 500N is required for ISMA to be performed for medium sized machines. The APCID design must be able to support its own weight and maintain its stability when such high impact forces are applied. Therefore, the design criteria for a high impact force and a stable support is given the highest relative importance.

In real life industry applications, medium sized machines come in a variety of sizes and dimensions and are confined in small rooms with limited room to maneuver. Therefore, the upscaled APCID design needs to have multiple axis and direction impact force with an adjustable height and span to reach for impacting of hard to reach places and irregular surfaces. As such, these design requirements are given a medium level of relative importance.

The portability of the upscaled APCID is taken into consideration as machines are to ease the process of transportation from one machine room to another. As such, a lightweight design is vital to facilitate the portability of the upscaled design. A compact design is also preferred to ease the storage process of APCID when not in use. From the literature reviews, the design requirements of a safe, portable, and robust upscaled APCID are tabulated in Table 4.1 with its relative importance.

Table 4.1: Upscaled APCID design requirements and its relative importance

Item No.	Design Requirement	Relative Importance
1	High impact force between 200N to 1000N	5
2	Stable statically and dynamically	5
3	Impart impact force in multiple axis	3
4	Adjustable height	3
5	Adjustable span	3
6	Ease of portability	1
7	Lightweight	1
8	Compact design	1

Universiti Malaya

4.2.2 Concept Generation

Based on the design requirements, 3 unique design concepts of the upscaled APCID are generated and a weighted selection matrix is used to evaluate these concepts.

Concept 1

Concept 1 is a cantilevered beam design that overhangs the solenoid on one end of the beam with extendable legs as shown in Figure 4.1. A steel box enclosure to house batteries is located at the base to act as counterweight. The solenoid is mounted on a slidable trolley with U-clamp to allow for adjustable span and impacts in multiple axis. A telescopic supporting stem with clamp allows for height adjustments when required. This allows for adjustable height and extendable span for imparting impacts at different location of the medium sized industrial machine.

In fully extended configuration, the overall dimension of the design is 1390 x 420 x 1025 mm (L x W x H). When folded, the overall dimension is reduced to 700 x 420 x 820 mm (L x W x H). This small footprint allows for the upscaled design to fit into the narrow service space between pumps which are usually 600mm wide. This option allows for separation of the APCID into 2 modular parts for easy transporting and maneuvering. Moreover, casters and handles are included in the design for easy movement and lifting of the APCID that weighs 30kg.

Universiti Malaya

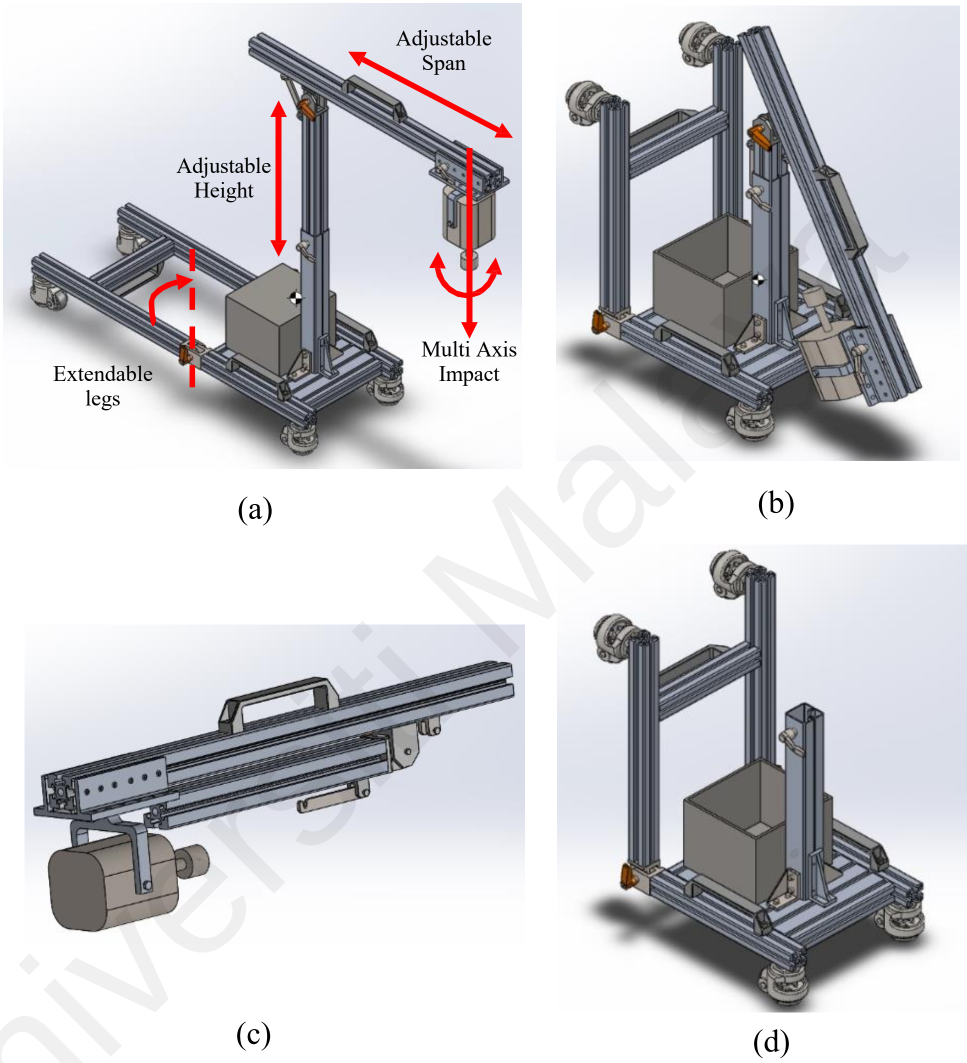

Figure 4.1: Concept 1 in (a) fully extended configuration, (b) folded configuration, (c) top modular part and (d) bottom modular part

Universiti Malaya

Concept 2

Concept 2 is a cantilevered beam design that overhangs the solenoid on one end of the beam with foldable legs as shown in Figure 4.2. The other end of the beam is connected by a link to the base support for additional stability. A steel box enclosure to house rechargeable batteries located at the T-base acts as counterweight. The solenoid is mounted on a slidable track with U-clamp to allow for adjustable span and impacts in multiple axis. The telescoping allows for adjustable height to reach different impact location. This allows for adjustable height and extendable span for imparting impacts at different location of the machine.

In fully extended configuration, the overall dimension of the design is 1220 x 450 x 910 mm (L x W x H). When folded, the overall dimension is reduced to 600 x 450 x 890 mm (L x W x H). This small footprint allows for the upscaled design to fit into the narrow service space between pumps which are usually 600mm wide. This option allows for separation of the APCID into 2 modular parts for easy transporting and maneuvering. Casters and handles are included in the design for easy movement and lifting of the APCID that weighs 37kg.

Universiti Malaya

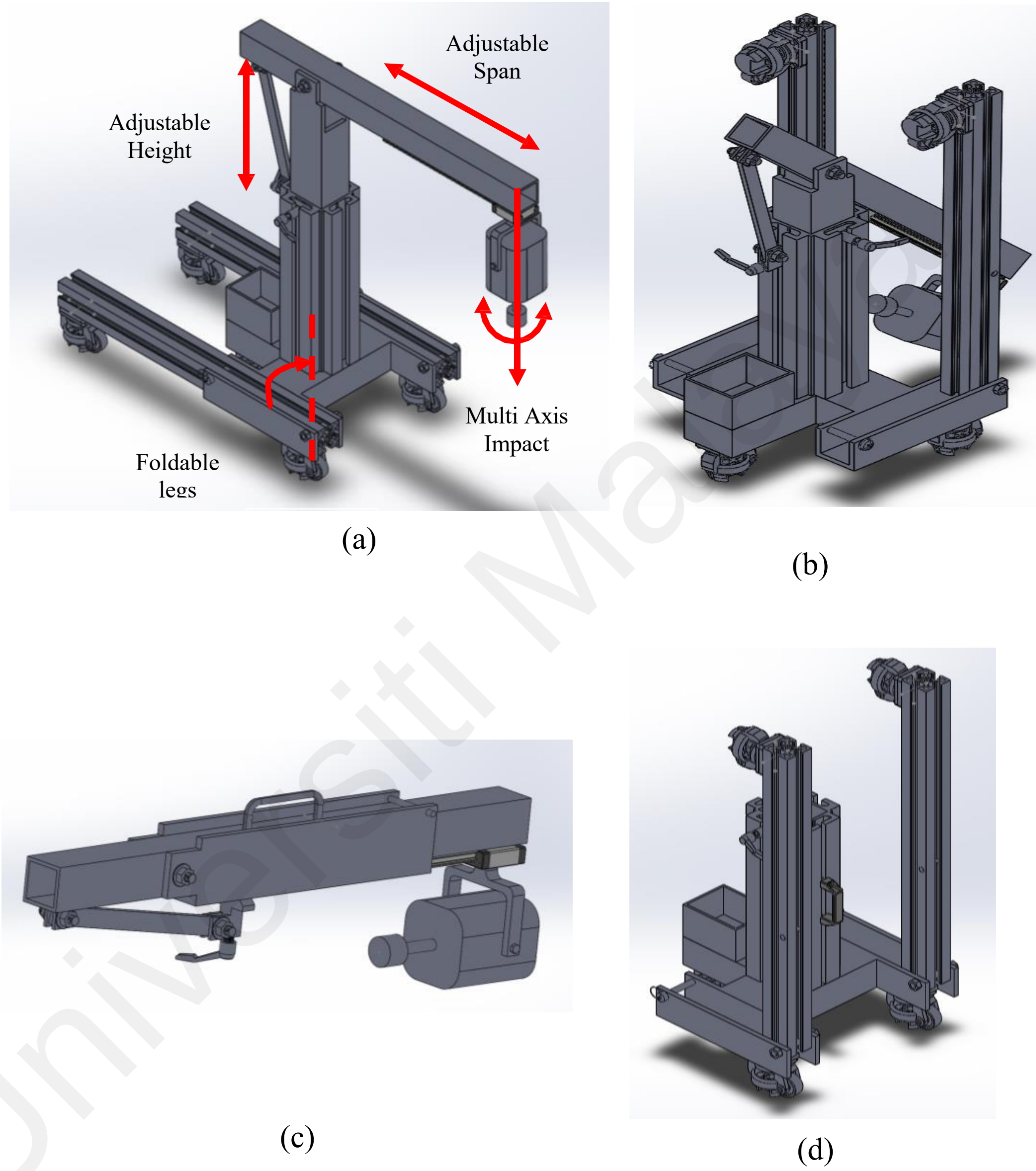

Figure 4.2: Concept 2 in (a) fully extended configuration, (b) folded configuration, (c) top modular part and (d) bottom modular part

Concept 3

Concept 3 is a horizontal beam design that is supported on both ends which are bolted to a steel plate as shown in Figure 4.3. This design mounts the solenoid on a slidable trolley with U-clamp for adjustable span and impacts in multiple axis. The rechargeable batteries can be placed on the steel plate for extra stability. The supports are made of aluminium profile of fixed length that slides against each other for height adjustments. A notch cut out on the bottom steel plate so that the machine can be located directly below the solenoid for vertical impacts.

In fully extended configuration, the overall dimension of the design is 1000 x 400 x 1200 mm (L x W x H). When folded, the overall dimension is reduced to 1000 x 600 x 200 mm (L x W x H). This option is a one-piece design which does not allow for separation into modular parts. However, the supports are designed to be collapsible to make a compact design which use a spring latch to ease the folding and assembly process.

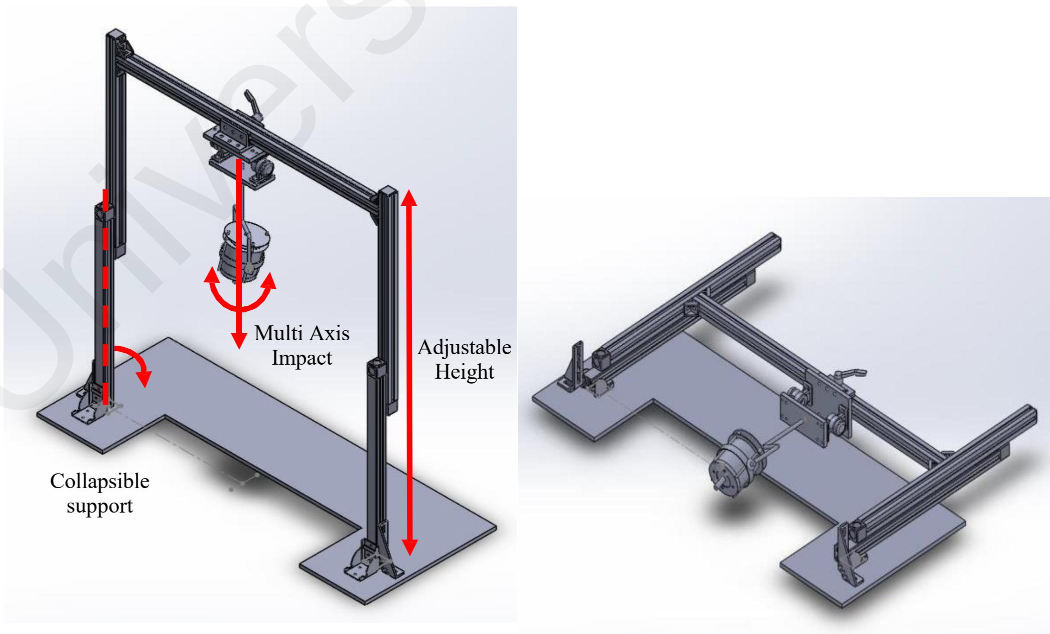

(a) (b)

Figure 4.3: Concept 3 in (a) fully extended and (b) folded configurations

Universiti Malaya

4.2.3 Concept Selection

The 3 concepts are evaluated using a weighted selection matrix and results are tabulated in Table 4.2. The weightage of each criteria is based on its relative importance identified from the previous section with the highest importance given a 20% weightage and the medium importance of 15% weightage and the lowest importance a 5% weightage. Based on the scoring obtained, concept 1 is noted to have the highest total weighted score of 4.70, followed by Concept 2 at 4.35, and Concept 3 with the lowest score of 4.20.

Table 4.2: Concept design selection matrix

Design Criteria	Weight	Concept 1		Concept 2		Concept 3	
		Rating	Score	Rating	Score	Rating	Score
High impact force	20%	5	1.00	5	1.00	5	1.00
Stability	20%	4	0.80	4	0.80	5	1.00
Multi-axis impact	15%	5	0.75	5	0.75	5	0.75
Height adjustability	15%	5	0.75	3	0.45	4	0.60
Span adjustability	15%	5	0.75	5	0.75	4	0.45
Portability	5%	5	0.25	5	0.25	2	0.10
Weight	5%	4	0.20	3	0.15	1	0.05
Compactness	5%	4	0.20	4	0.20	5	0.25
Total Weighted Score		**4.70**		**4.35**		**4.20**	
Ranking		**1**		**2**		**3**	

As all 3 concepts uses the same high impact producing solenoid and is mounted on a U-clamp for multi-axis impact, the scores are similar for these factors. In terms of stability, concept 3 scored the highest as it has the lowest center of gravity due to its high weight and largest base area compared to the other concepts. In terms of height adjustability, concept 1 scored the highest as it has the greatest range of adjustability of 400 mm followed by concept 2 with 380mm and concept 2 with 350mm. As concept 3 has limited span adjustability, it scored the lowest among the 3 concepts.

Universiti Malaya

As casters and handles are used in concept 1 and 2 and the design is separable into two modular components, the highest score is given for both of them as the designs are very portable. As concept 1 has the lowest weight, the design is awarded the highest score in this category. In terms of compactness, concept 3 scored the highest as its dimensions reduces the most when folded for storage.

As such, concept 1 scored the highest overall as it satisfies the design requirement for a stable APCID design for high impact force usage. It is also the lightest design with desirable features for modal analysis testing such as adjustable height, span and modular components. Hence, concept 1 s selected to be further developed in the following stage

4.3 Design Development Phase

The concept design selected is developed in the phase with further information and details. Suitable materials and parts are reviewed and selected according to the design needs. Detailed drawings are then created to finalized the design and dimension of the upscaled APCID. Computational analysis is conducted on the 3D model developed to determine the structural integrity of the device.

4.4 Detailed Design

Concept 1 is developed further with information on its material and parts required. Suitable solenoids and materials for the APCID support are compiled and evaluated. Detail drawings in 2D and 3D are produced with its dimension and material used. Bill of material of the APCID is then generated to ease the procurement and fabrication process of the upscaled APCID.

4.4.1 Solenoid Selection

In order to impart a higher impact force between 200 N to 500 N, a stronger solenoid with more coil windings are required As the battery used as the power source supplies voltage at 42V, 4 different commercially available solenoids that generates a high impact force at this voltage are identified from Geeplus are compared in Table 4.3.

Table 4.3: Comparison of solenoid properties

Model	870C	870F	874C	874F
Operating Voltage (V)	19 – 60	19 – 60	25 – 80	25 – 80
Weight (kg)	1.885	1.885	3.000	3.000
Dimension, D x H (mm)	87 x 47	87 x 47	87 x 82	87 x 82
Stroke (mm)	14	10	30	14
Holding Force at 10% ED (N)	200 - 900	150 - 2000	70 - 1000	200 - 2000
Cost (RM)	600	600	1100	1100

Model 874F is selected to be used as it produces the highest impact force within the desired range of 200N to 500N has a reasonable dimension and weight. The cost of the selected model is slightly more expensive but still affordable.

4.4.2 Detailed Drawings

Based on the finalized concept, the 3D model is created, dimensioned and assembled in Solidworks. The concept consists of two modular components, namely the top part and bottom part. 3D perspective views and 2D detailed drawings with the front, top and side view of the assembly and modular components are extracted from the 3D model created are presented from Figure 4.4 to Figure 4.7. The overall dimension of the concept design is found to be 1390 x 420 x 1025 mm (L x W x H) and 700 x 420 x 820 mm (L x W x H) for fully extended and folded configurations respectively. The range of the span, ℓ was designed to be 600mm and the maximum height, h achieved is 700mm. The solenoid can be rotated freely for a range from 0º to 180º in all 3 directions, θx, θy and θz.

Universiti Malaya

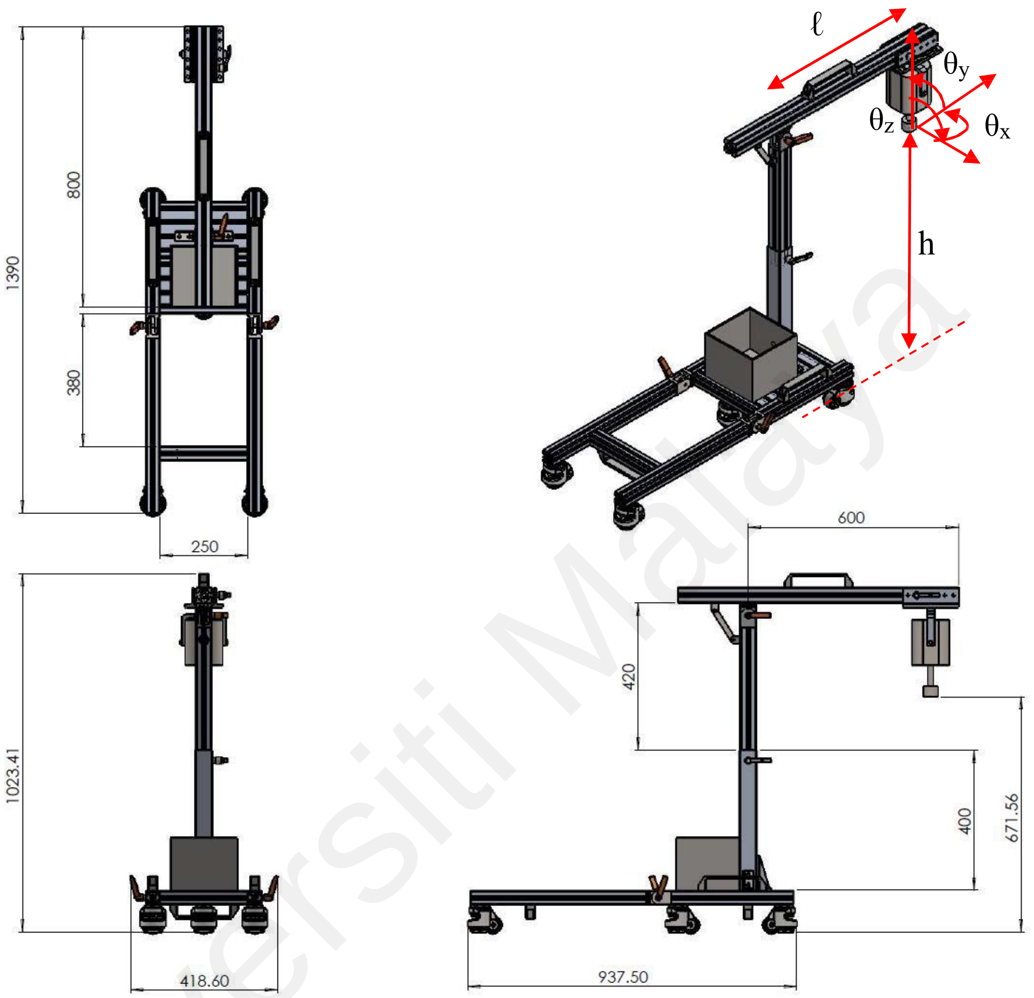

Figure 4.4: Isometric view and orthogonal projection of fully extended upscaled APCID

Universiti Malaya

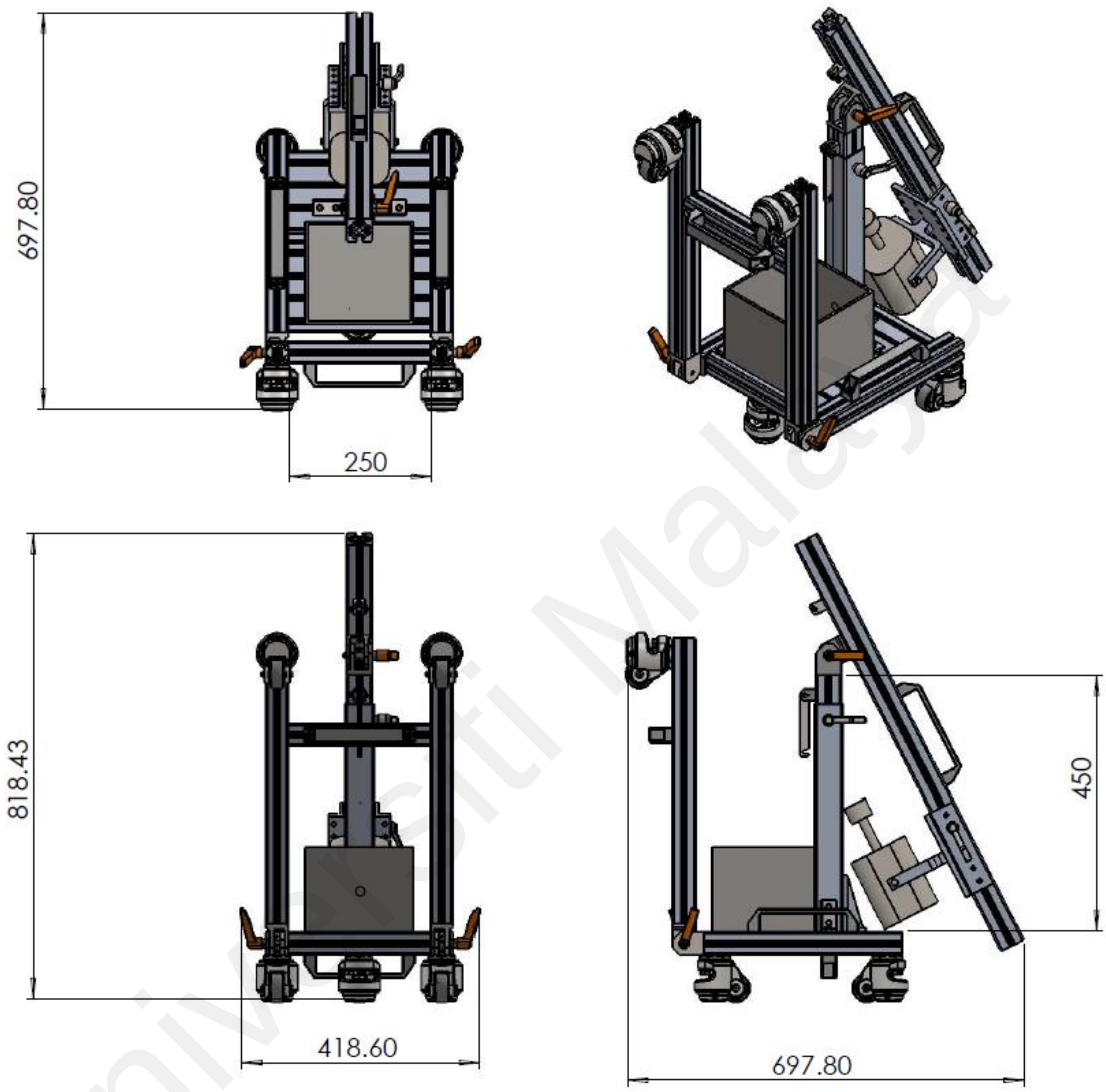

Figure 4.5: Isometric view and orthogonal projection of folded upscaled APCID

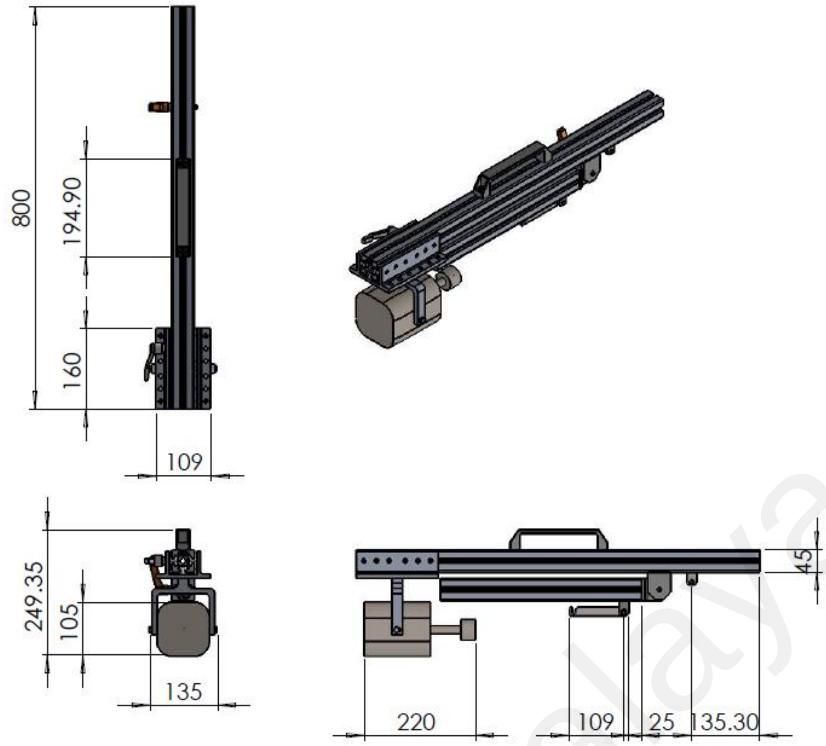

Figure 4.6: Isometric view and orthogonal projection of top modular part

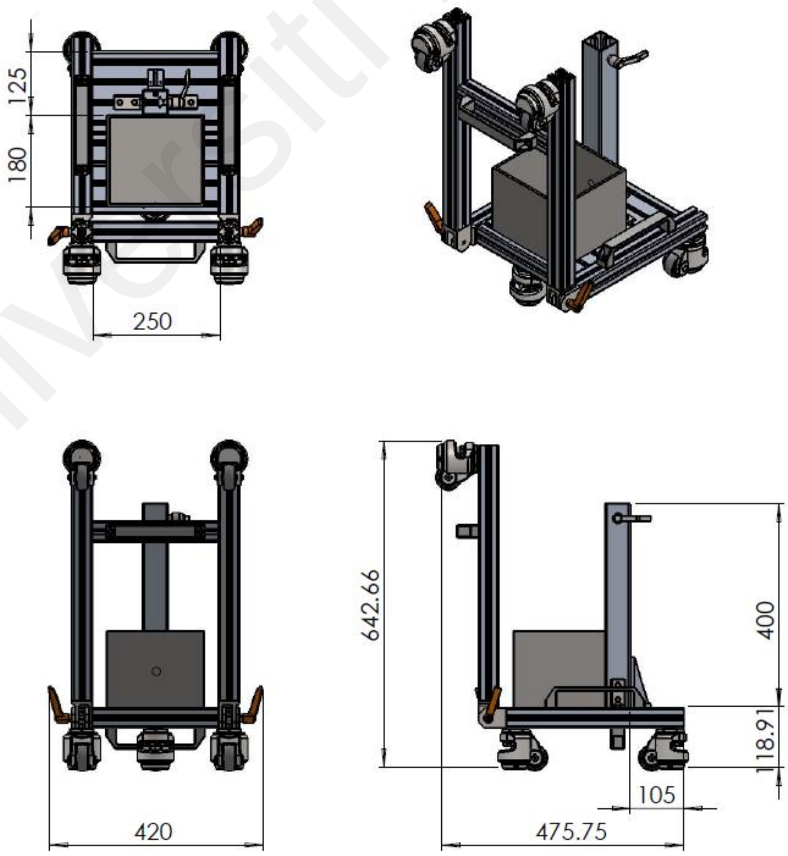

Figure 4.7: Isometric view and orthogonal projection of bottom modular part

Universiti Malaya

4.4.3 Material Selection

The material selection is a process of selecting the most suitable material for the fabrication of the upscaled APCID. Aluminium alloy and structural steel are the main materials used as they are strong and durable materials suitable to support the upscaled APCID. The properties of these materials are tabulated and compared in Table 4.4.

Table 4.4: Material properties comparison of aluminium alloy and structural steel

Properties	Aluminium Alloy	Stainless Steel
Tensile Yield Strength (MPa)	241	275
Density (g/cm^3)	2.71	7.85 – 8.06
Ease of Fabrication	Easy	Medium
Corrosion Resistance	High	High
Relative Cost	Low	High

Aluminium alloy and stainless steel are both corrosion resistant materials with high tensile yield strength with stainless steel being slightly stronger. However, the density of aluminium alloy is 3 times less dense than stainless steel and thus weighing significantly lesser than stainless steel. As aluminium is comparatively softer than stainless steel, it is a material that is easier to be drilled and manipulated during the fabrication process. Moreover, the cost of aluminium alloy is also relatively lower than stainless steel.

Therefore, the main material selected for the main structure of the upscaled APCID is aluminium alloy. This is to ensure the design is as lightweight as possible to improve its portability and ease of transportation. However, stainless steel is also used for components which are subjected to a higher amount of stress such as the angle joints, connection link and hinges. This improves the strength and safety factor of the upscaled APCID with a minimal cost increment as these parts are relatively small. The bill of material of the upscaled APCID are tabulated in Table 4.5.

Universiti Malaya

Table 4.5: Bill of material of upscale APCID

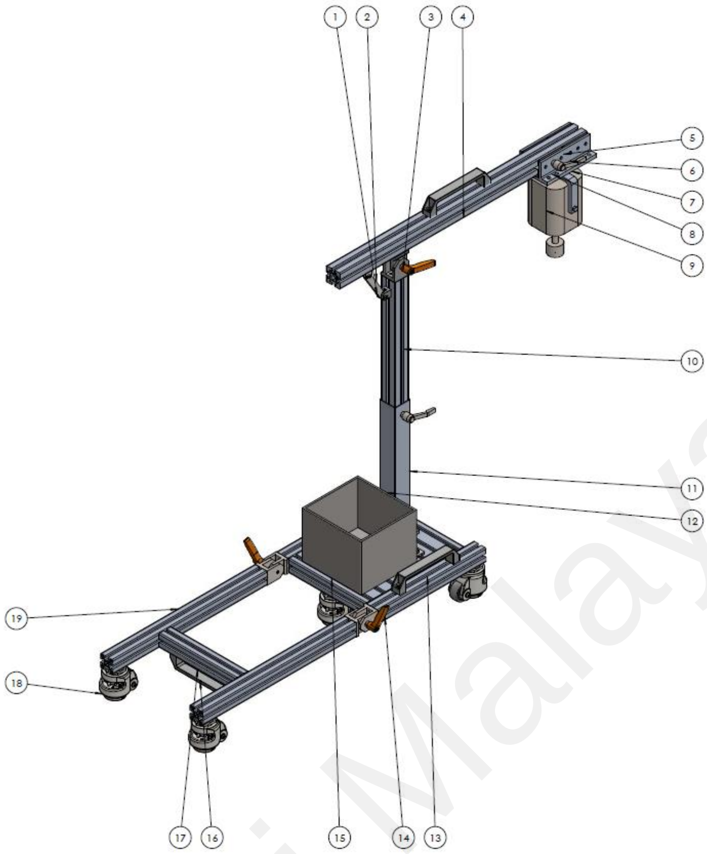

No.	Description	Qty	Material
1	Hinge	2	Stainless Steel
2	Connection link	1	Stainless Steel
3	45 x 45mm Angle joint with clamp	1	Aluminium Alloy
4	45 x 45mm T-slot Aluminium profile (800mm)	1	Aluminium Alloy
5	Slider Block	4	PVC
6	Clamp Lever	2	Stainless Steel
7	Slider Trolley	1	Aluminium Alloy
8	Solenoid Bracket	1	Stainless Steel
9	Solenoid	1	Stainless Steel
10	45 x 45mm T-slot Aluminium profile (400mm)	1	Aluminium Alloy
11	50 x 50mm Hollow Aluminium Profile	1	Aluminium Alloy
12	Battery enclosure	1	Stainless Steel
13	40 x 40mm T-slot Aluminium profile (350mm)	2	Aluminium Alloy
14	40 x 40mm Angle joint with clamp	2	Aluminium Alloy
15	45 x 160mm T-slot Aluminium profile (250mm)	2	Aluminium Alloy
16	Handle	3	Aluminium Alloy
17	40 x 40mm T-slot Aluminium profile (250mm)	1	Aluminium Alloy
18	Caster with stopper	5	PVC
19	40 x 40mm T-slot Aluminium profile (500mm)	2	Aluminium Alloy

Universiti Malaya

4.5 Computational Analysis Result

The computational analysis results consist of 5 sections, namely toppling, static, dynamic, modal frequency and shape and harmonic response analyses. The results obtained are presented and discussed in the following sections.

4.5.1 Toppling Analysis

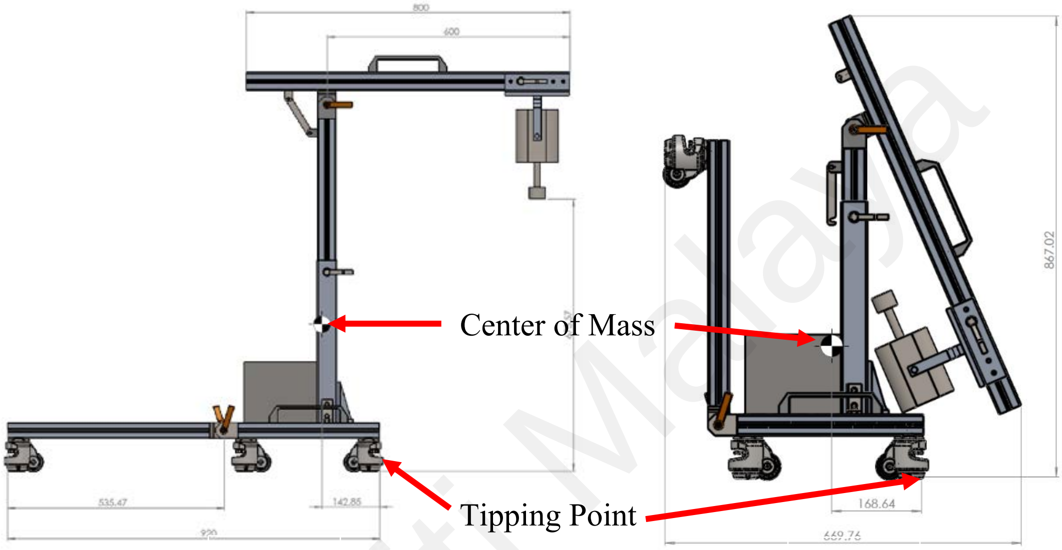

(a) (b)

Figure 4.8: Center of mass and tipping point of (a) fully extended and (b) folded configuration

Toppling analysis is carried out to determine the stability of the APCID design and they are presented in Figure 4.8. The center of mass is a point in space where the total weight of the APCID is assumed to act at while the tipping point is the point or edge nearest to the center of mass. The center of mass is 143mm away and 169mm away from the tipping point for the fully extended and folded configuration respectively.

This center of mass is nearer to the tipping point in the fully extended configuration as the solenoid's weight is acting outside of the base footprint. The center of mass is also slightly higher in this configuration as the total height is higher than the folded configuration. Nonetheless, the upscaled APCID is stable in both fully extended and folded configurations as the center of mass is located before its tipping point.

Universiti Malaya

4.5.2 Static Analysis

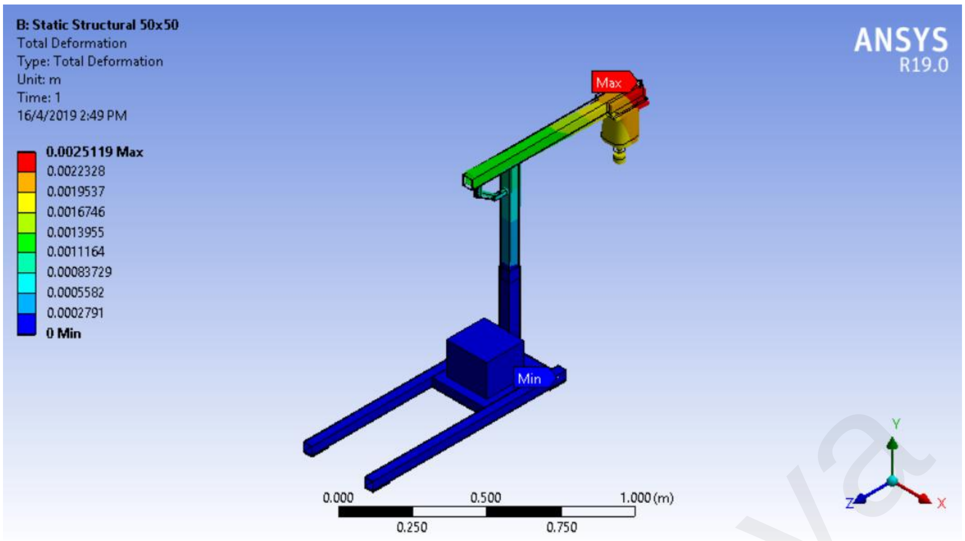

(a) Total deformation

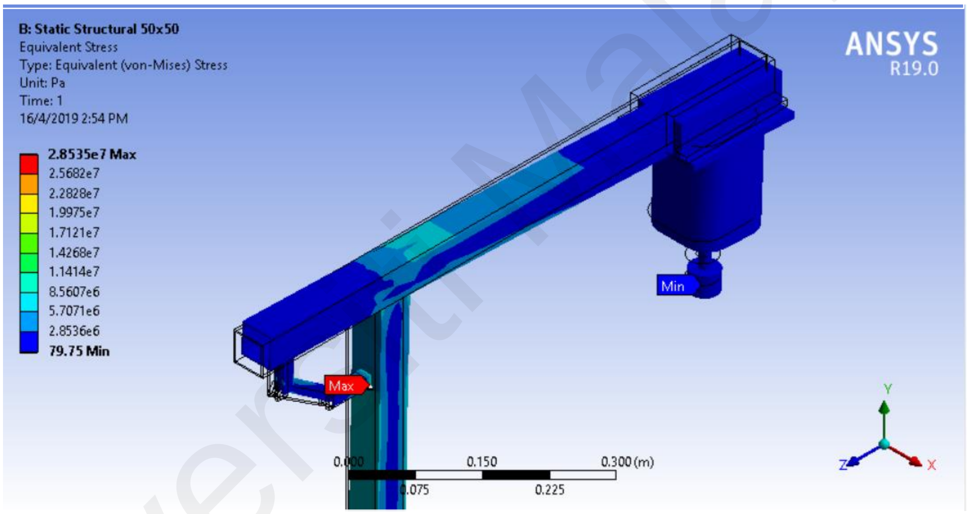

(b) Maximum equivalent von Mises stress

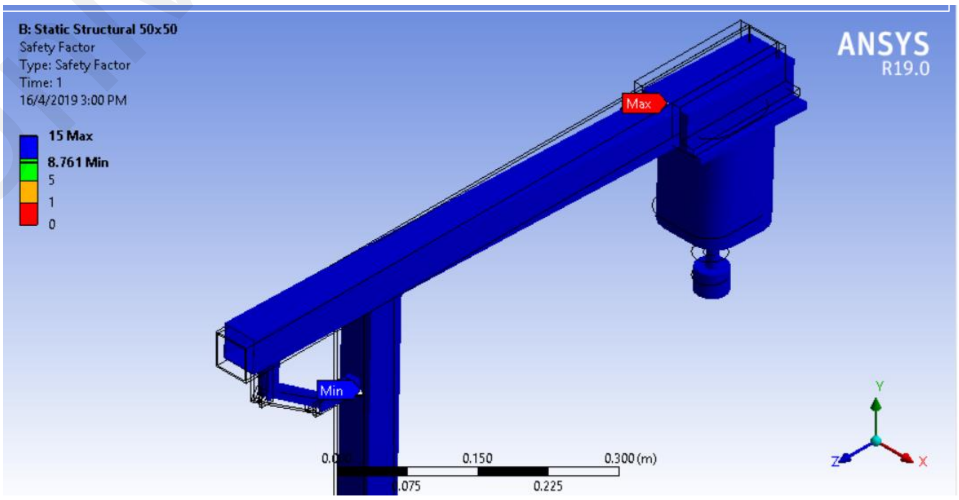

(c) Static safety factor

Figure 4.9: Total deformation, equivalent stress and static safety factor of static analysis

Universiti Malaya

For static analysis, the total deformation, equivalent stress and safety factor are determined as shown in Figure 4.9. The horizontal beam is observed to deflect downwards by a maximum of 2.5119 mm at the end of the beam. The supporting stem is also noted to be bent forward slightly. These minor deflections caused by the weight of the overhanging solenoid are relatively small compared to the dimensions of the APCID and thus deemed acceptable.

The maximum equivalent stress is observed to be 28.535 MPa and is located at the hinge connection with the supporting stem. This tensional stress is caused by the reaction forces used to counter the bending of the horizontal beam. The safety factor at this location is calculated to be 8.761 using maximum equivalent von Mises stress theory. As the safety factor is well above 1, it is deduced that static failure will not occur as the structural integrity of the APCID remains intact statically.

4.5.3 Dynamic Analysis

The dynamic response due to a transient impact force is evaluated and presented in Figure 4.10 . A transient impact force of 800N is applied at the tip of the solenoid at 0.1s for a duration of 0.01s which is similar to a typical impact force. The total deformation of horizontal beam and supporting stem is observed to oscillate and decay over time due to the impulsive force. The maximum deflection of 29.24 mm is noted at the end of the horizontal beam at 0.15s, which is immediately after the application of impact force.

The maximum equivalent von Mises stress of 23.58 MPa is also observed at 0.15s, which is immediately after the impact force application and decays with time. This stress is located at the hinge linking the beam to the supporting stem. This is due to the tensional reaction forces induced to counter the bending motion of the horizontal beam. As the safety factor is calculated to be 1.0599, the upscaled APCID design will not fail.

Universiti Malaya

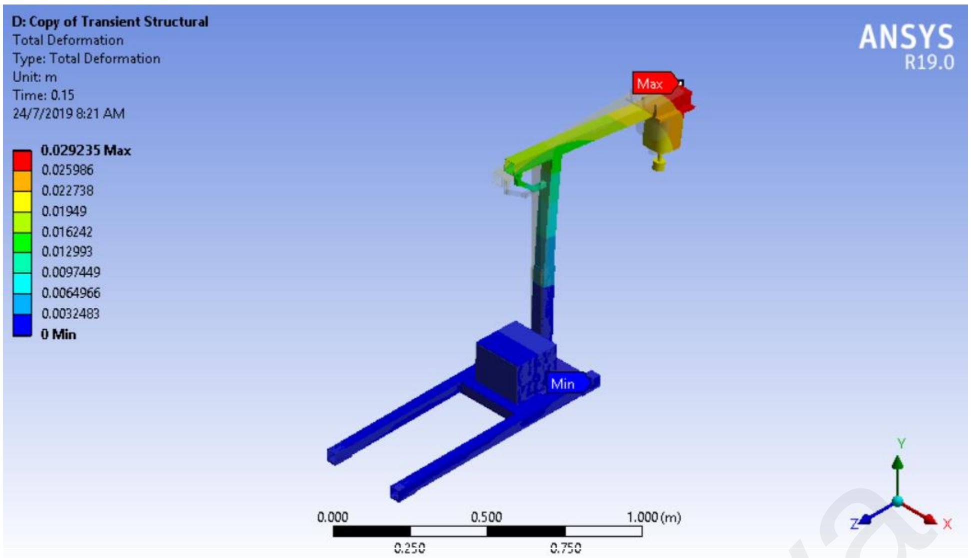

(a) Total deformation

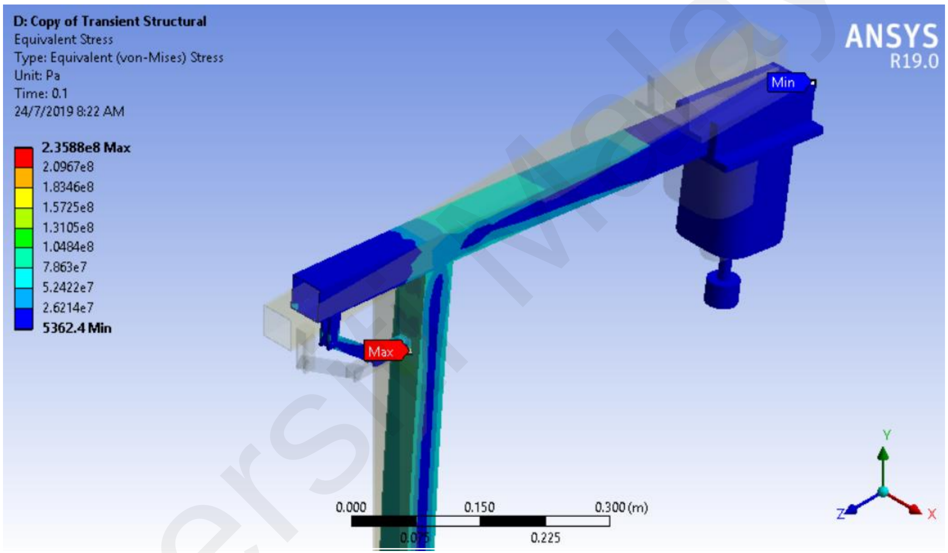

(b) Maximum equivalent von Mises stress

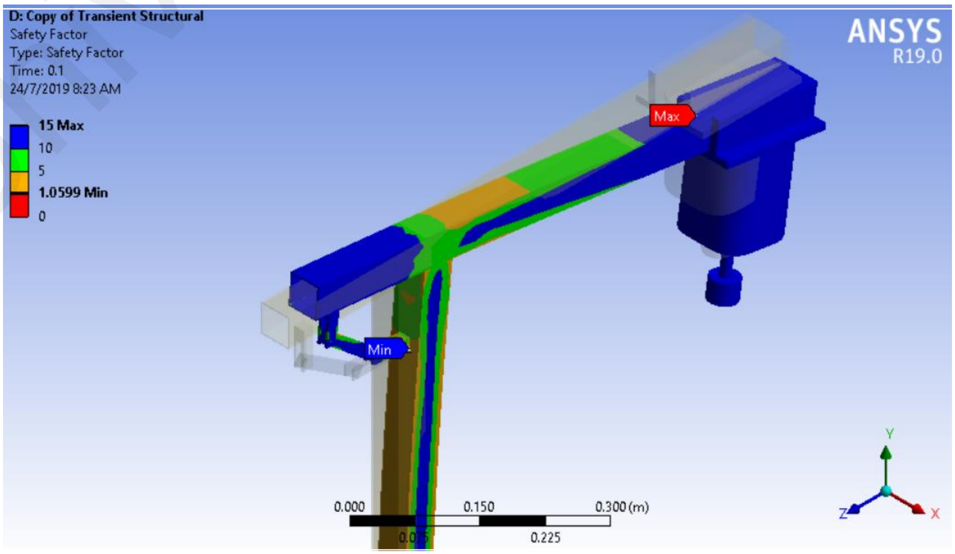

(c) Static safety factor

Figure 4.10: Total deformation, equivalent stress and static safety factor of dynamic analysis

Universiti Malaya

4.5.4 Modal Analysis

Modal analysis is performed on the upscaled APCID to identify its natural frequency and mode shapes. This is important in order to understand and predict the behavior of the structure during resonance due to harmonic excitations. The first 5 mode shapes and its corresponding mode shapes determined are tabulated in Table 4.6.

Table 4.6: Natural frequencies and corresponding mode shapes of upscaled APCID

Mode	Total deformation of APCID	Natural Frequency	Mode shape
1	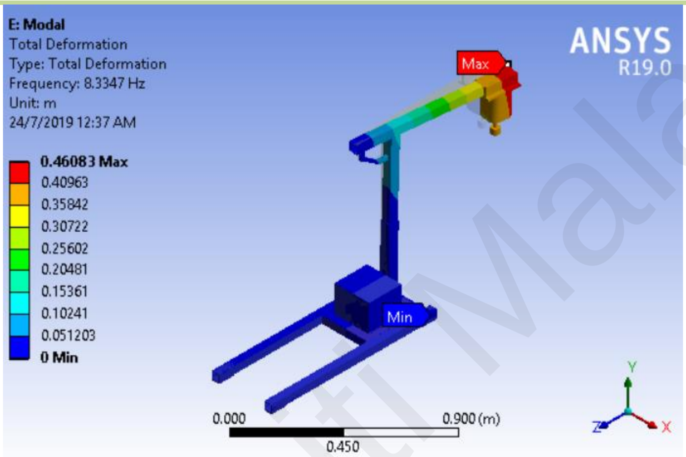	8.3347 Hz	Bending of beam in x direction
2	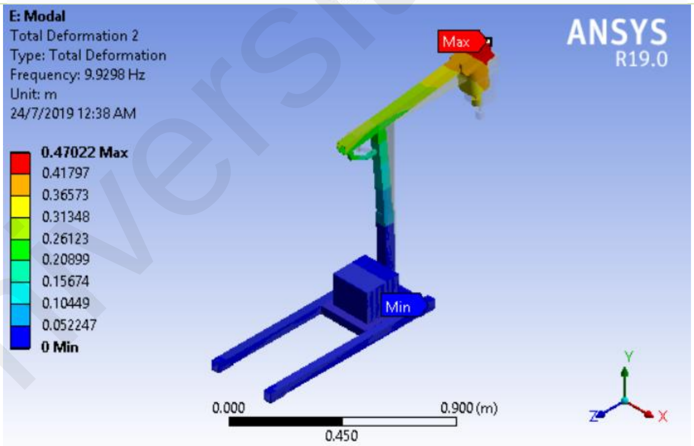	9.9298 Hz	Bending of beam in y direction
3	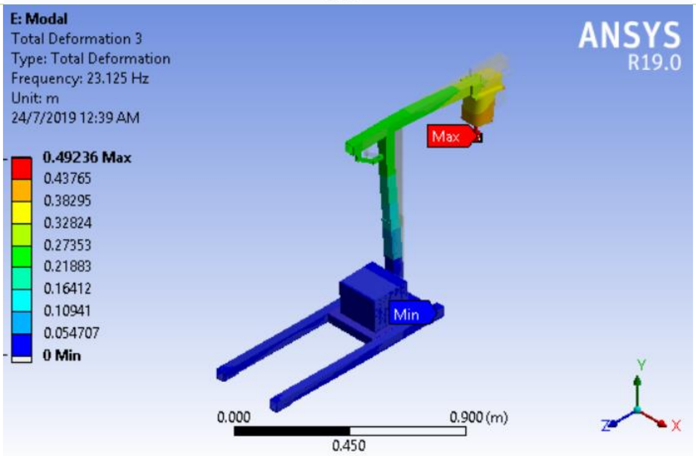	23.125 Hz	Bending of beam in z direction

Universiti Malaya

Table 4.6 continued

Mode	Total deformation of APCID	Natural Frequency	Mode shape
4	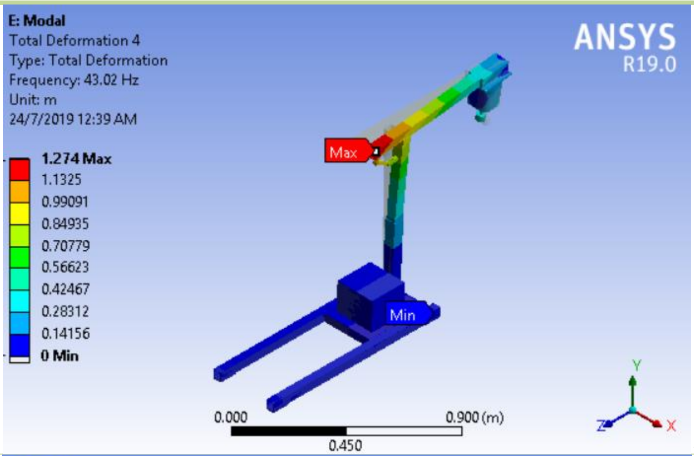	43.02 Hz	Bending of support in x direction
5	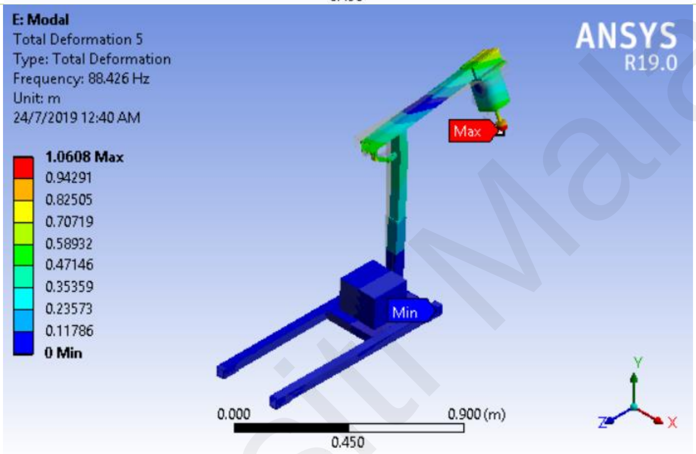	88.426 Hz	Bending of beam and stem in x direction

The operating speed of medium sized industrial machines commonly ranges between 0 Hz to 100Hz. Based on the modal analysis results, it was found that 5 natural modes exist within this range as shown in Table 4.6. The first 5 modes found are of bending shape in different directions. Mode 1, 4 and 5 resonates by in the x-direction at 8.3347 Hz, 43.02 Hz and 88.426Hz respectively. Meanwhile, mode 2 resonates in the y-direction at 9.9298 Hz and mode 3 in the z-direction at 23.125 Hz.

As the APCID is mounted on the floor, harmonic excitation force received from the vibrating machine in operation will act vertically in the y-direction. As such, mode 2 at 9.9298 Hz is expected to contribute dominantly to the response as other modes are not excited by the base excitation. Therefore, mode 2 is the main concern of this study as resonance may occur if the base is excited at frequencies near its natural frequency.

Universiti Malaya

4.5.5 Harmonic Response Analysis

Harmonic response analysis is carried out to determine the response of the upscaled APCID design when subjected to a harmonic excitation. As the device is mounted on the floor, machines in operation will transfer some of its vibrations to it through the floor with a velocity of less than 4mm/s. As resonance is likely to be at mode 2, a harmonic force of velocity 4mm/s is swept through frequencies from 5 to 15 Hz to study the deformation and stress induced. The frequency response graph of amplitude and phase angle generated is as shown in Figure 4.11

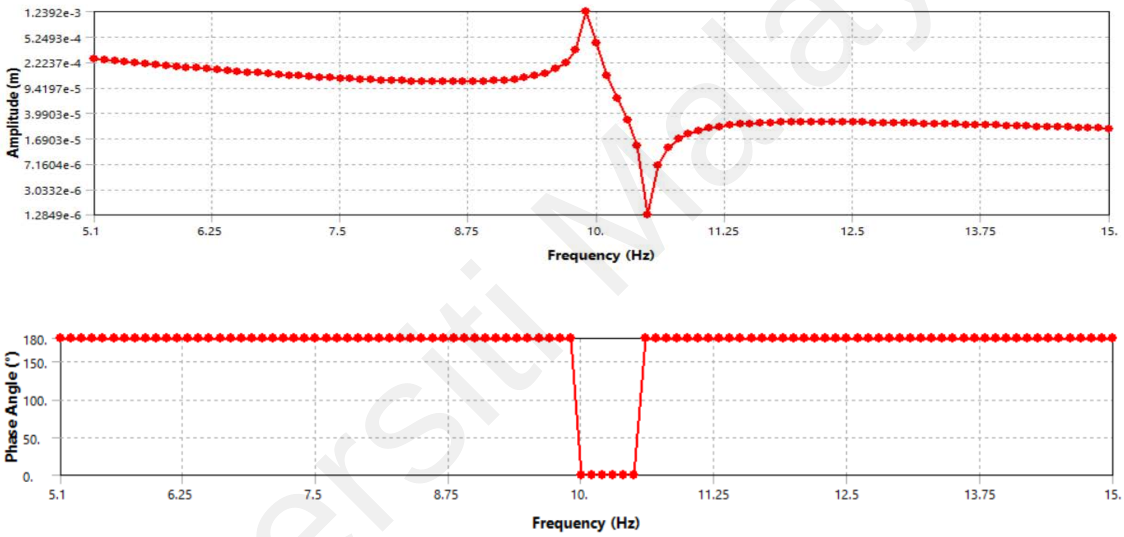

Figure 4.11: Frequency response graph of amplitude and phase angle vs frequency

It is observed that the APCID is in resonance at 9.9Hz as the amplitude is the highest at this point and a 180° change in phase angle occurred. This is because frequency is very close to the natural frequency of mode shape 2. Therefore, the harmonic responses at 9.9 Hz presented in Figure 4.12 are the maximum responses. The maximum total deformation is found to be 10.5mm located at the furthest end of the horizontal beam. The maximum equivalent stress of 85.888Mpa is located at the hinge connecting the beam and the supporting stem. This results in a minimum fatigue safety factor of 1.0069 for a design cycle of 100000 cycles. Therefore, the design is considered safe and resonance due to harmonic excitation of the base will not cause failure easily.

Universiti Malaya

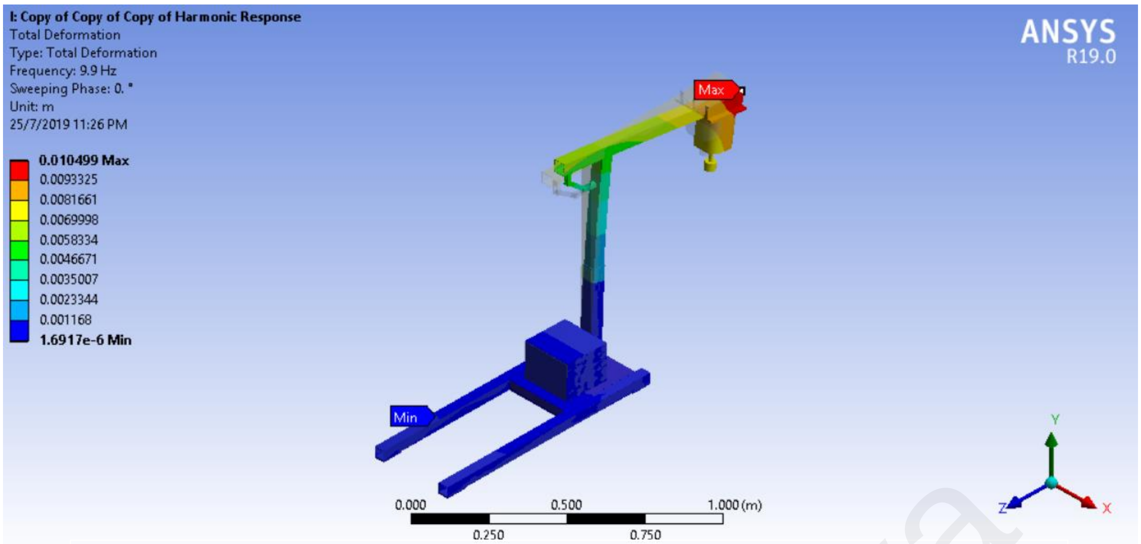

(a) Total deformation

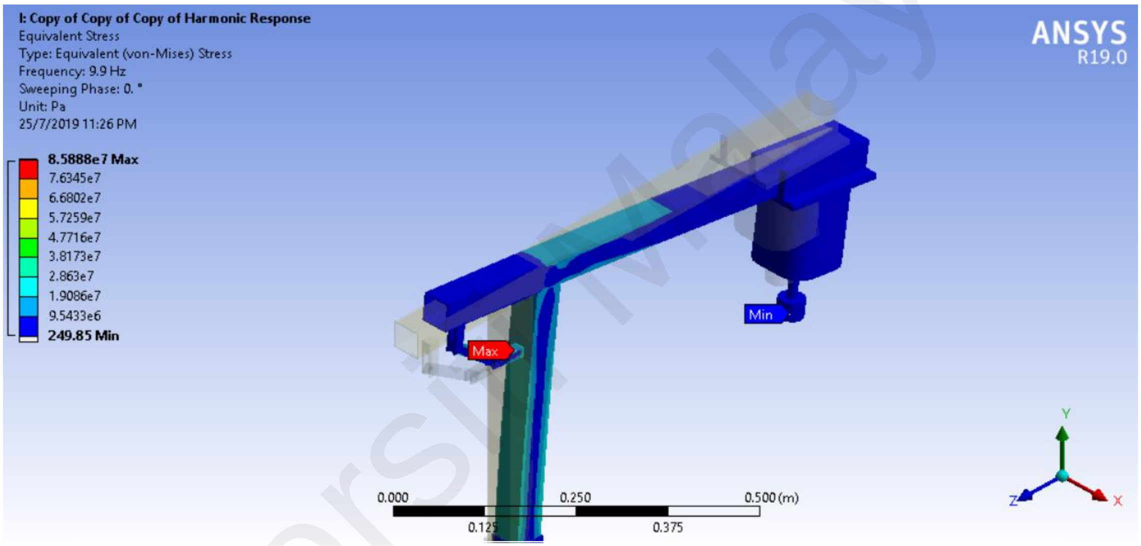

(b) Maximum equivalent von Mises stress

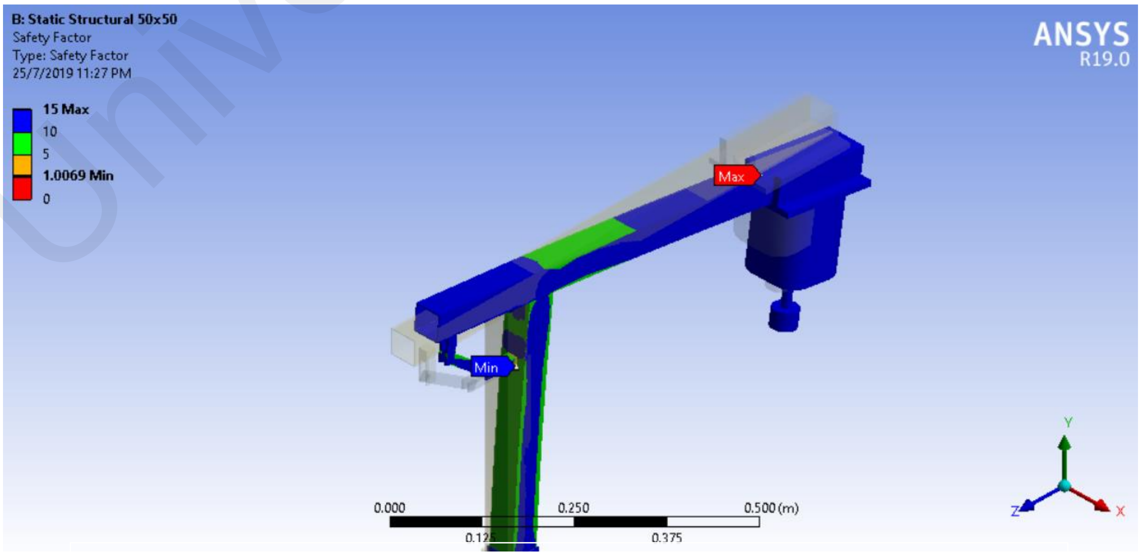

(c) Fatigue safety factor

Figure 4.12: Total deformation, equivalent stress and fatigue safety factor of harmonic response analysis

Universiti Malaya

4.6 Fabrication of APCID

The fabrication process of a functional upscaled APCID is discussed in detail here.

4.6.1 Cost Estimation

In order to fabricate the APCID, an estimated budget is compiled using the Bill of Materials developed. The cost of each part required is based on a market survey from at least three local suppliers and the lowest cost is selected. The sum of all these costs are then tabulated in Table 4.7 and the required budget is found to RM 5,070.00.

Table 4.7: Estimated budget cost of APCID

No.	Description	Qty	Unit Cost	Total Cost
1	Hinge with pin	2	150.00	300.00
2	Connection link	1	120.00	120.00
3	45 x 45mm Angle joint with clamp	1	100.00	100.00
4	45 x 45mm T-slot Aluminium profile (800mm)	1	92.00	92.00
5	Slider Block	4	2.50	10.00
6	Clamp Lever	2	55.00	110.00
7	Slider Trolley	1	225.00	225.00
8	Solenoid Bracket	1	184.00	184.00
9	Solenoid model 874F	1	1,100.00	1,100.00
10	45 x 45mm T-slot Aluminium profile (400mm)	1	46.00	46.00
11	50 x 50mm Hollow Aluminium Profile	1	48.00	48.00
12	Battery enclosure	1	300.00	300.00
13	40 x 40mm T-slot Aluminium profile (350mm)	2	33.00	66.00
14	40 x 40mm Angle joint with clamp	2	108.00	216.00
15	45 x 160mm T-slot Aluminium profile (250mm)	2	93.00	186.00
16	Handle	3	47.00	141.00
17	40 x 40mm T-slot Aluminium profile (250mm)	1	25.00	25.00
18	Caster with stopper	5	290.00	1450.00
19	40 x 40mm T-slot Aluminium profile (500mm)	2	47.00	47.00
20	L Brackets	3	11.00	33.00
21	Rechargeable Battery	1	240.00	240.00
22	Nuts and bolts	1 Lot	31.00	31.00
Total Budget				5,070.00

Universiti Malaya

4.6.2 Prototype Assembly

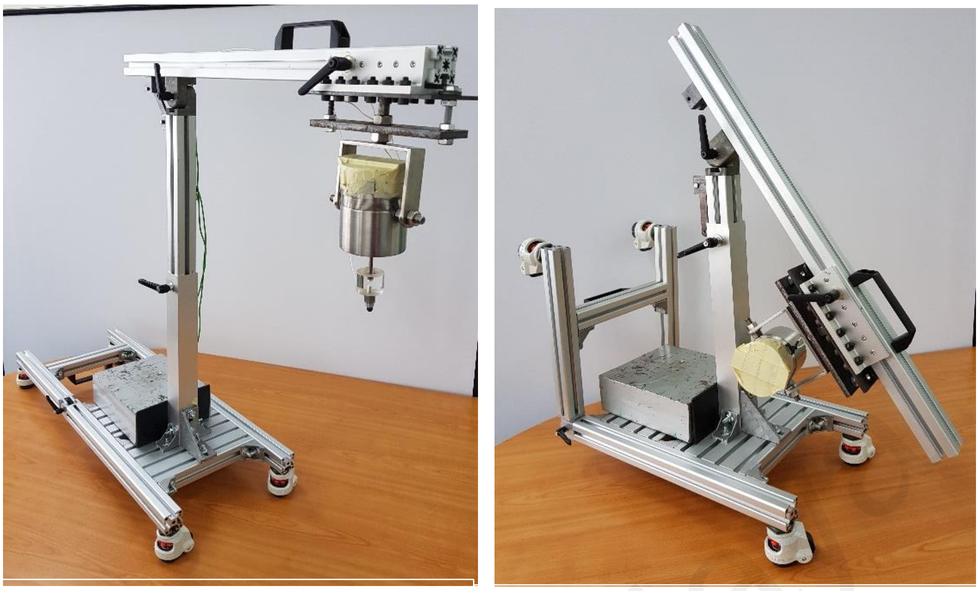

(a) (b)

Figure 4.13: APCID prototype in (a) fully extended and (b) folded configuration

The materials and components procured are assembled together to make the prototype upscaled APCID. The assembled prototype in fully extended and folded configurations shown in Figure 4.13 are similar to the developed detail drawings of Concept 1. A laptop containing the LabVIEW control system is connected to the solenoid and placed on the battery housing as shown in Figure 4.14 to complete the working prototype.

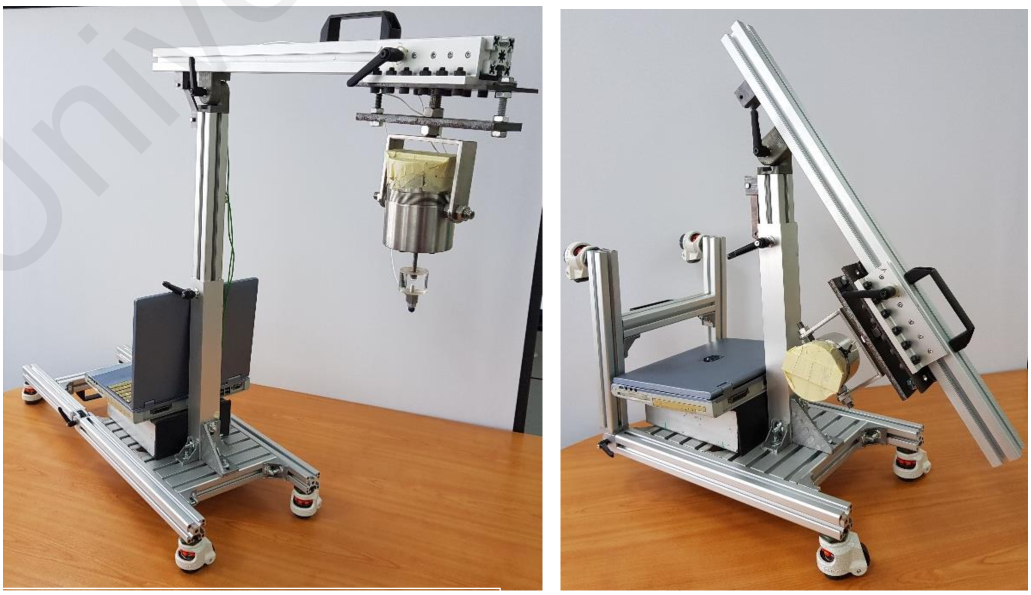

(a) (b)

Figure 4.14: APCID with control system in (a) fully extended and (b) folded configuration

Universiti Malaya

(a)

(b)

Figure 4.15: Modular parts of prototype. (a) top part and (b) bottom part

When separated to be transported, the modular parts of the fabricated prototype are shown in Figure 4.15. The prototype is found to be stable even without the battery counterweight as shown in both figures above. The upscaled APCID design assembled is very similar to the 3D model created in Solidworks shown in Figure 4.4 to Figure 4.7.

The total weight of the APCID is found to be 32kg which is very similar to the designed weight. The top modular part is weighs 14 kg while the bottom modular part weighs 18kg. The additional weight may be due to inaccuracies during cutting and drilling of materials and additional materials used such as nuts and bolts added to secure components in place.

When the adjustable rubber stopper of the casters is lowered down fully, the wheels are lifted above the ground to prevent any movement of the upscaled APCID. During impacts, the APCID remains stationary as the friction forces between the rubber and the floor surfaces are higher than the reaction forces of the impacts. These acts as fixed supports which are similar to the fixed boundary conditions used in the computational analysis. The adjustable height and span are found to be 400mm and 700mm which are similar to the designed values. The U-clamped allows the solenoid to be rotate and locked in the desired direction in all 3 degrees of freedom as designed. Therefore, a functional prototype of an upscaled APCID is successfully fabricated for ISMA testing.

Universiti Malaya

4.7 Recalibration of Upscaled APCID

The impact forces of the upscaled APCID is recalibrated to achieve a similar impact force profile generated by lab-scale APCID. As shown in Figure 4.16, the impact force generated by the upscaled APCID is 12 times higher than the lab-scale APCID and has the same profile of a sharp distinctive peak that occurs over a short period of time. Therefore, the upscaled APCID has successfully enlarged the impact force while maintaining a smooth impact profile similar to the lab-scale APCID.

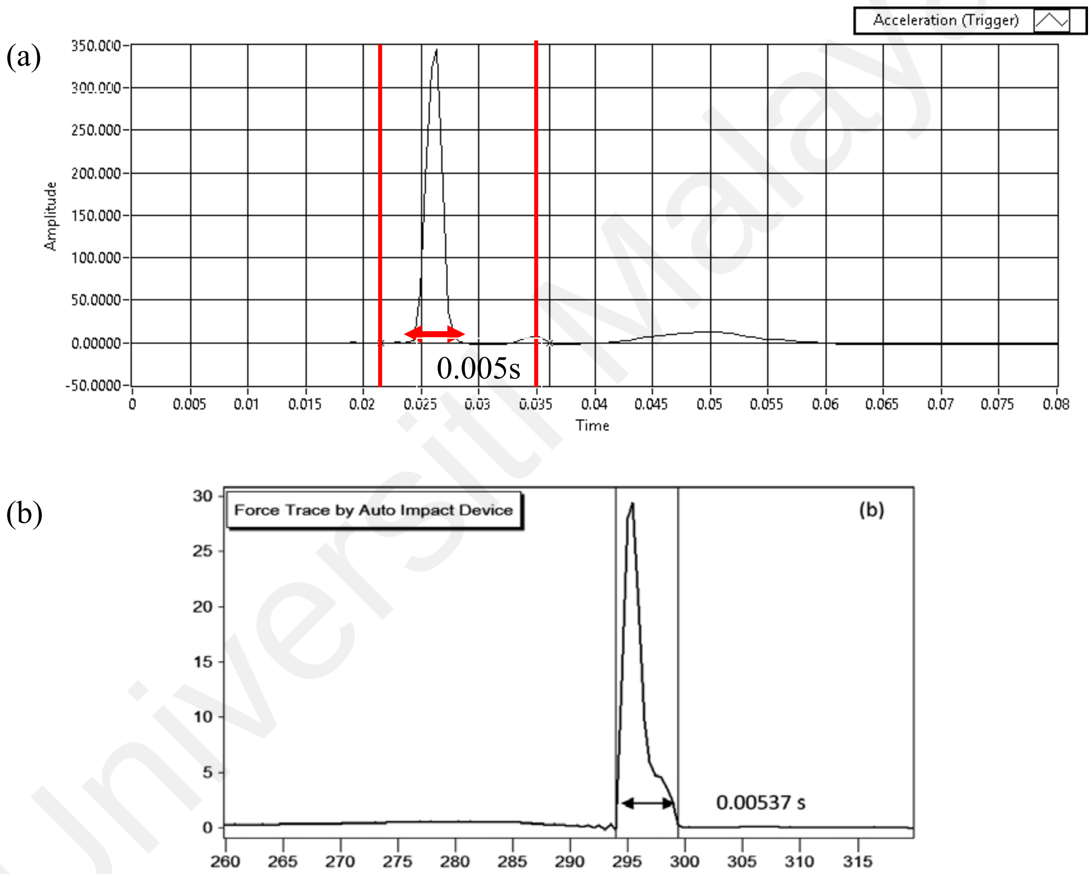

Figure 4.16: Comparison of impact profile of (a) large scale APCID of 345N for 0.005s and (b) lab-scale APCID of 28N for 0.00537s

The upscaled APCID are then recalibrated to maximize the impact force while maintaining the smoothness of the impact profile. The is achieved by varying the solenoid voltage, activation time and separation distance of the force transducer and the impact surface. The optimum settings of these parameters to generate a high impact force and smooth impact profile are investigated in the following sections.

4.7.1 Voltage Level of Solenoid

The impact force is measured as the voltage supplied to the solenoid is varied between 26V to 48V. The separation distance is kept at 7mm with an activation time of 50ms for both vertical impact and horizontal impact forces. The results are tabulated in Table 4.8 and a graph of impact force against voltage level is plotted in Figure 4.17.

Table 4.8: Vertical and horizontal impact force at different voltage level

Voltage (V)	Vertical Impact Force (N)	Horizontal Impact Force (N)
26	154.324	-
28	180.810	-
30	220.072	-
32	213.64	22.189
34	225.005	101.458
36	233.106	167.128
38	238.637	230.721
40	248.637	269.228
42	259.001	316.719

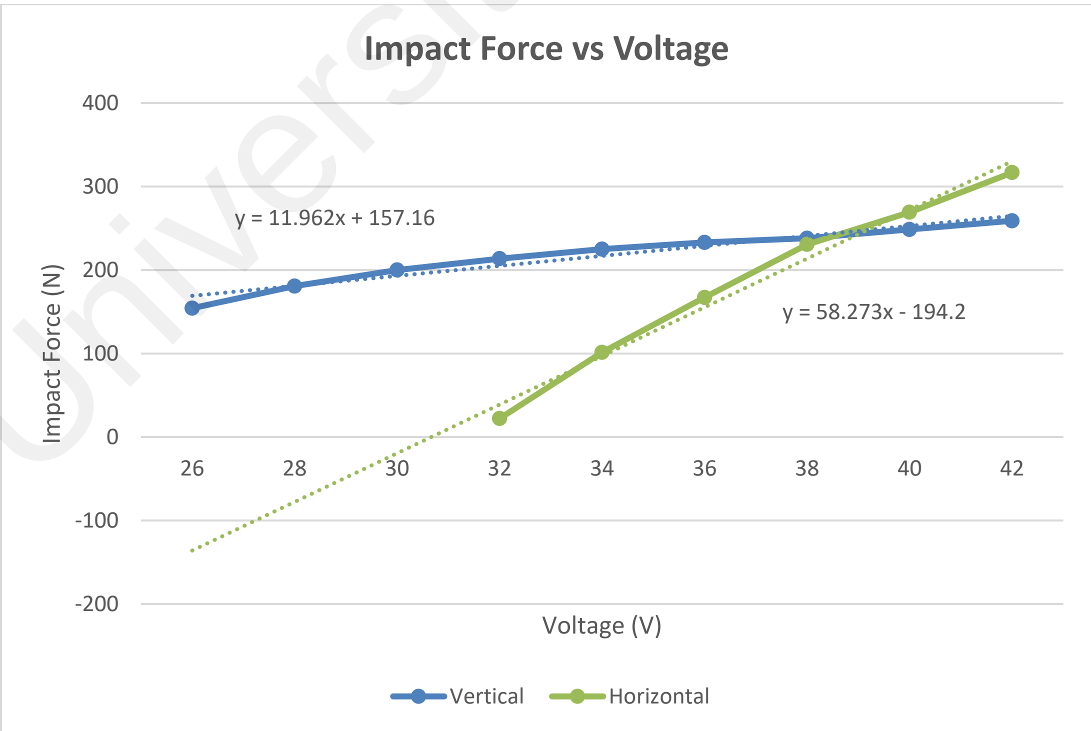

Figure 4.17: Graph of impact force against voltage level supplied to solenoid

Universiti Malaya

In both scenarios, the impact force increases proportionally with the increase of voltage level supplied. This is because an increase in voltage creates a higher electromagnetic force in the coil windings of the solenoid which in turn generates stronger pushes on the plunger. A linear line of best fit is applied on the data collected as shown in Figure 4.17 which can be used to control the desired impact force by varying the voltage level supplied. For voltages below 38V, the impact force of vertical impacts is larger than horizontal impacts while at voltages above 38V, the horizontal impact force is larger. This is because the impact force increases at a higher rate for horizontal impacts compared to vertical impacts as the gradient of horizontal impacts trendlines are larger.

4.7.2 Solenoid Activation Time

The activation time refers to the amount of time the solenoid is energized. The separation distance is kept at 7mm with a voltage level of 42 V which is similar to the voltage of the batteries used. This activation time is controlled using LabVIEW and varied from 50ms to 65ms which is based on the range of activation time settings used for lab-scale APCID to achieve a good impact profile (Lim et al., 2018a). The results for vertical and horizontal impacts are tabulated in Table 4.9 and a graph of impact force against activation time is plotted in Figure 4.18.

Table 4.9: Vertical and horizontal impact force at different activation time

Activation Time (ms)	Vertical Impact Force (N)	Horizontal Impact Force (N)
50	254.412	316.719
55	258.041	331.964
60	251.657	329.162
65	249.514	321.642

Universiti Malaya

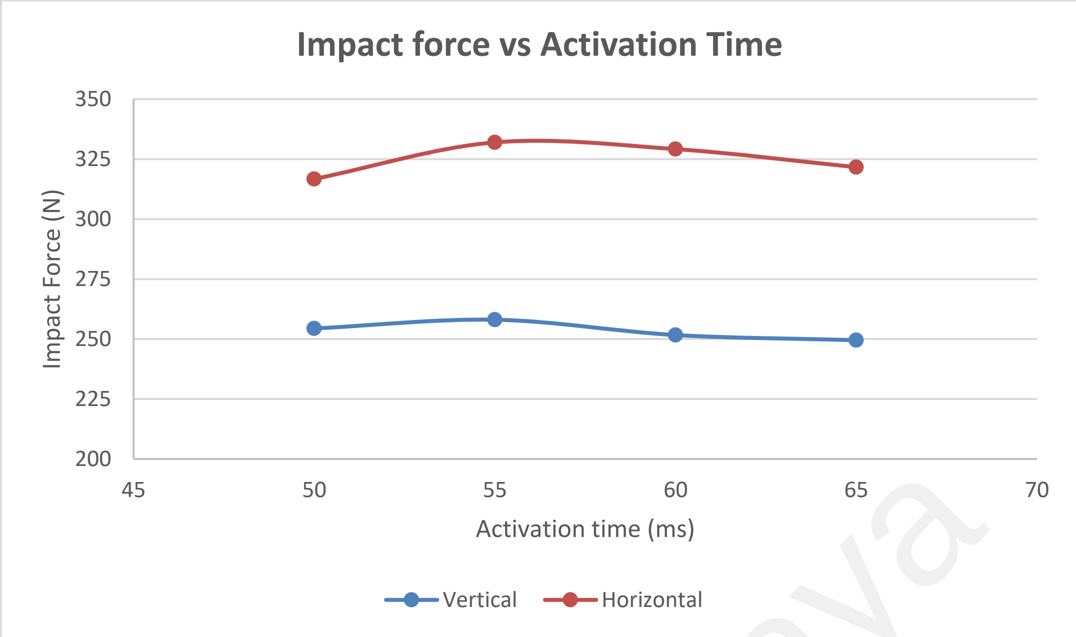

Figure 4.18: Graph of impact force against activation time of solenoid

Based on the results, it is observed that as the activation time increases the impact force generated increases to a certain limit and then reduces. This is because as activation time increase, the solenoid pushes the plunger for a longer period thus increases the impact force and stroke length. However, the increase in impact force will be limited by the separation between the plunger and the surface of impact where any additional force is used to deform the surface and it is no longer considered as an impact force. For both horizontal and vertical impact cases, the optimum activation time to create a maximum impact force is 55ms.

4.7.3 Separation Distance

The separation distance refers to the space between the top of the force transducer to the impact surface. This separation distance needs to be calibrated to ensure the sufficient distance is allowed for the plunger to travel to impart the impact force. The voltage is set at 42V which is similar to the battery source used and the activation time is kept at 50ms for both horizontal and vertical impact cases. The results obtained are tabulated in Table 4.10 and a graph of impact force against separation distance is plotted in Figure 4.19.

Universiti Malaya

Table 4.10: Vertical and horizontal impact force at different separation distance

Separation Distance (mm)	Vertical Impact Force (N)	Horizontal Impact Force (N)
5	242.67	216.857
6	299.665	264.052
7	259.702	324.564
8	200.705	346.297
9	123.982	230.731

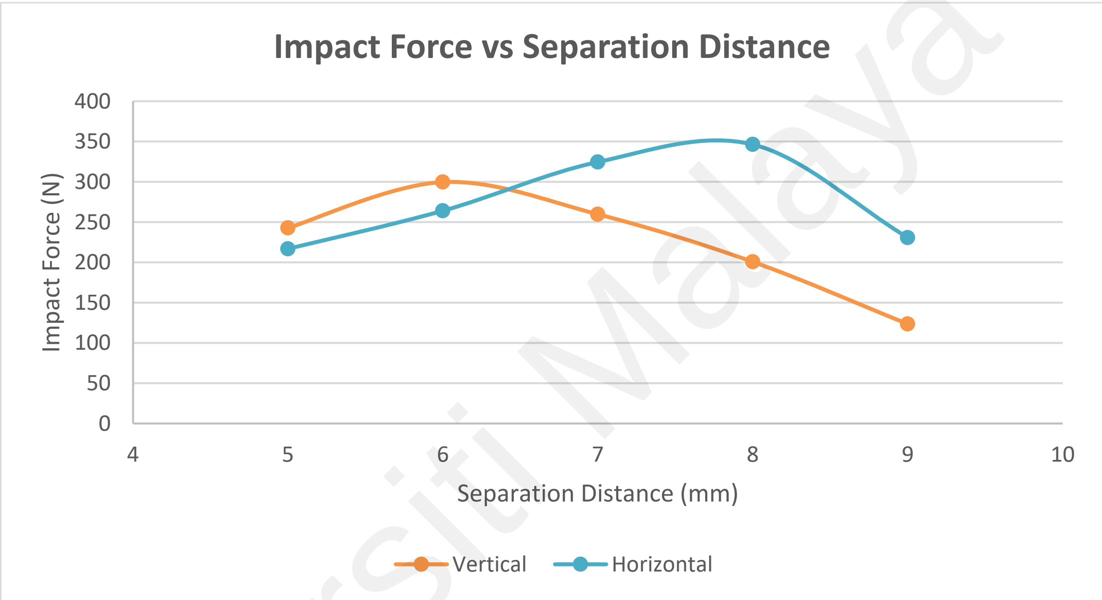

Figure 4.19: Graph of impact force against separation distance of impact surface

Although the highest vertical impact force is obtained at 6mm, the impact profile is not as smooth as the 7mm impact profile shown in Figure 4.20 as the force level fluctuates significantly after the impact is made. This is because as the activation time is prolonged, the solenoid is energized for a longer time and thus resulting in a longer stroke. However, at small separation distance, the motion of the plunger is limited and the high impact force deforms the impact surface. Therefore, the optimum separation distance for vertical impacts is 7mm to impart an impact force of 259.702N with a good impact profile. For horizontal impacts, the smooth profile is obtained at 8mm with an impact for of 346.297N as shown in Figure 4.21.

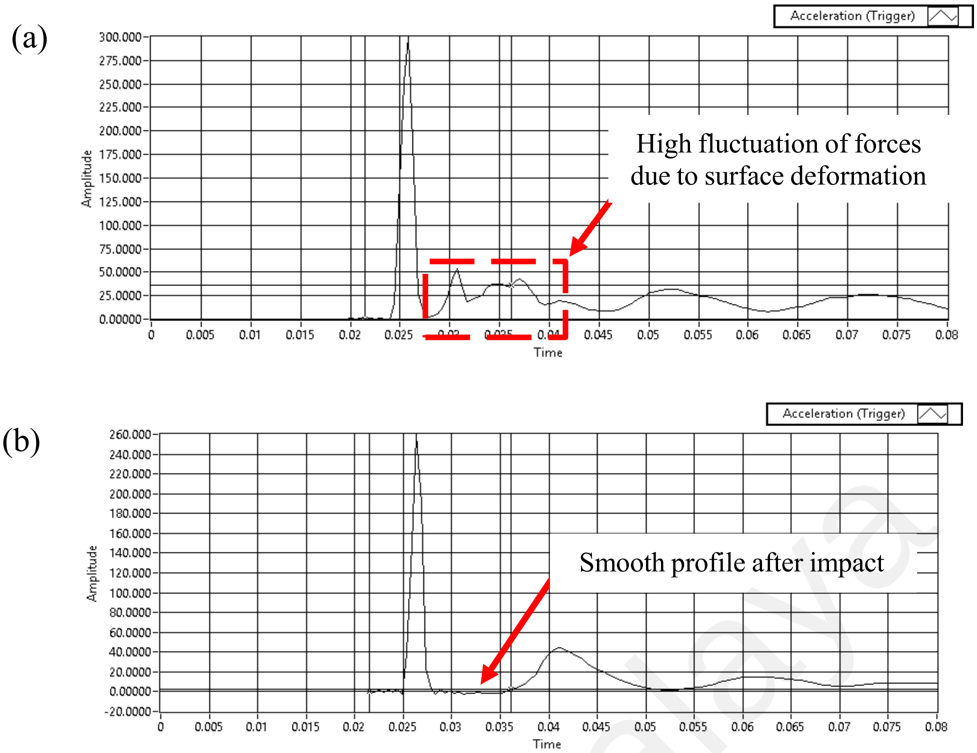

Figure 4.20: Comparison of smoothness of vertical impact profile for (a) 6mm and (b) 7mm separation distance

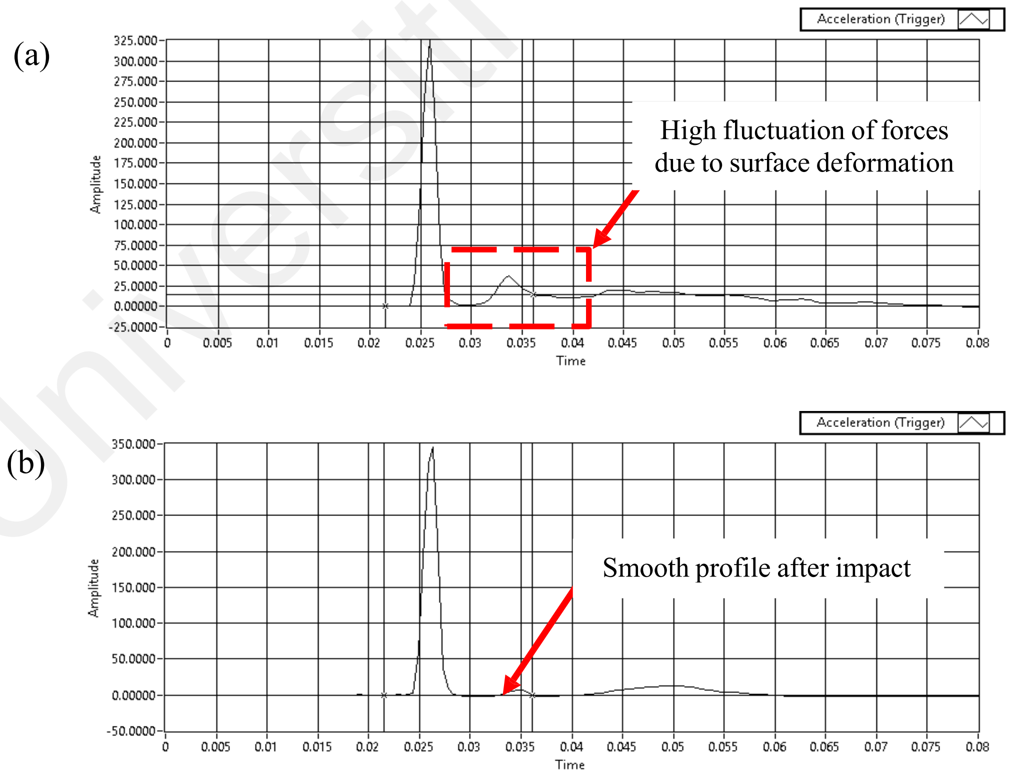

Figure 4.21 Comparison of smoothness of horizontal impact profile for (a) 7mm and (b) 8mm separation distance

Universiti Malaya

From the result obtained, it is observed that an optimum separation distance exists between the force transducer and the impact surface to generate a maximum impact force. As the separation distance increase, the impact force increases until a certain limit and then decreases for both cases. As the distance increases, the plunger travels a longer stroke to impart an impact on the surface. This causes more energy is lost to compress the return spring further thus resulting in a lower impact force. Hence, the optimum separation distance for vertical impacts and horizontal impacts are 7mm and 8mm respectively.

4.8 Summary

The results of the conceptualization, design development and implementation phase has been presented and discussed thoroughly. In the conceptualization phase, 9 design requirements of an upscaled APCID is determined based on customer needs. 3 unique conceptual designs are generated and evaluated using a weighted selection matrix. concept 1 is selected as the concept design as it best satisfies all the design requirements.

In the design development stage, 2D and 3D drawings of the concept design is created with all the necessary information. Suitable materials and solenoids are sourced, and its properties compared in the material selection stage. ANSYS is used for computational analysis such as toppling, static, dynamic, modal and harmonic response analyses. The total deformation, maximum equivalent stress and safety factor are evaluated and discussed. Based on the results, the upscaled APCID designed is safe, reliable and robust as the safety factor is always more than 1 in all the analysis.

A budget cost estimate of RM 5,070 is compiled based on the bill of materials generated in the design development stage for procurement purposes. Upon procurement of the materials, a prototype of the upscaled APCID design is assembled. The total weight of 32kg which is similar to the simulated weight in 3D modelling. This prototype is then investigated for its working strategies to ensure that it functions as intended.

Universiti Malaya

The optimum settings for voltage, activation time and separation distance are determined by experiment. Generally, the impact force increases with the increase in voltage, activation time and separation distance. As the battery used as the portable power supplies a voltage of 42V, it is found that the optimum settings are 55ms for the activation time with a separation distance of 7mm and 8mm for vertical and horizontal impacts.

Using these settings, a good impact profile similar to the lab-scale APCID but with an increased impact force of 254.99 N and 346.297 N is obtained for vertical and horizontal impacts. The impact force lies within the targeted range of 200 N to 500 N and is suitable to be used for ISMA purpose on medium sized industrial machines. Hence, the upscaled APCID design is deemed suitable and acceptable.

Universiti Malaya

CHAPTER 5: CONCLUSION

5.1 Conclusion

The upscaled APCID design for ISMA is successfully designed with an enlarged impact force. The maximum impact force with a good impact profile is increased to 259.702 N and 346.297 N for vertical and horizontal impacts respectively. This is an enlargement of close to 9 times and 12 times as compared to the lab-scale APCID which provides an impact force of 28N with a good impact profile.

The structural integrity of the upscaled APCID design is evaluated the simulated results showed that the design is stable and safe. The static safety factors are found to be 8.761 for structural static analysis and 1.0599 for transient structural analysis. At 9.9 Hz which is close to the natural frequency of the design, the fatigue safety factor due to harmonic vertical base excitation is evaluated to be 1.0069 with a design life cycle of 1,000,000 cycles. As all the safety factors are above 1, the upscaled APCID design will not fail during operation and is considered to be a strong and sturdy design.

A functional upscaled APCID design prototype is fabricated based on the selected design. The design allows for adjustable height of up to 700mm and adjustable span of 600m suitable for medium sized industrial machines. The solenoid is mounted on a bracket that allows for 3 degrees of freedom for impacts to be imparted in horizontal, vertical and oblique directions The final assembly weighs 32kg and has an overall dimension of 1390 x 420 x 1025 mm (L x W x H) and 700 x 420 x 820 mm (L x W x H) for fully extended and folded configurations respectively.

The large scaled APCID is recalibrated by determining the optimum solenoid voltage level, activation time and separation distance impact to achieve the maximum impact force level with a good profile. As the battery used supplies a voltage of 42V, the optimum conditions are determined to be 55ms for activation time with a separation distance of

Universiti Malaya

7 mm for vertical impact force and 8mm for horizontal impact force. The maximum impact force imparted at these settings is 259.702 N and 346.297 N for vertical and horizontal impact conditions. These impact forces are within the desired range of 200N to 500N and is suitable to perform ISMA testing for medium sized industrial machines.

In conclusion, a large scale APCID is successfully designed, analyzed and fabricated for ISMA testing on medium sized industrial machines. The design is evaluated to be structurally intact and is supported with a stable and robust base. The prototype fabricated is similar to the 3D model and the relationships between the APCID impact force level with the solenoid voltage level, activation time and separation distance is also established.

5.2 Recommendations

The stability and structural integrity of the upscaled APCID can be improved in future works by introducing dampers to the design. These dampers can be attached to the casters to tune the harmonic excitations transmitted through the floor to the APCID. Therefore, the amplitude of resonance at mode 2 can be tuned down which in turn increases the fatigue safety factor and thus improves the robustness of the upscaled APCID.

Due to the limitation of commercially available solenoid, the impact force of the upscaled APCID is limited to be between 200 to 500N. This limits the application to medium sized industrial machines only. Therefore, a custom solenoid can be considered to increase the impact force to perform ISMA modal analysis testing on large sized industrial machines.

The APCID design can be further enhanced using stronger lightweight composite materials such as carbon fiber. This would improve the portability and structural integrity of the design. Due to limitation of resources, aluminium alloy was selected for this research project. Therefore, future studies can be conducted to study ways to reduce the weight of the upscaled APCID with strong lightweight materials to improve the design.

Universiti Malaya

REFERENCES

Cakir, F., & Uysal, H. (2015). Experimental modal analysis of brick masonry arches strengthened prepreg composites. *Journal of Cultural Heritage, 16*(3), 284-292. doi:https://doi.org/10.1016/j.culher.2014.06.003

Collinger, J. C., Wickert, J. A., & Corr, L. R. (2009). Adaptive Piezoelectric Vibration Control With Synchronized Switching. *Journal of Dynamic Systems, Measurement, and Control, 131*(4), 041006-041006-041008. doi:10.1115/1.3117189

Garcia-Perez, A., Amezquita-Sanchez, J., Dominguez - Gonzalez, A., Sedaghati, R., Osornio-Rios, R., & Romero-Troncoso, R. (2013). Fused empirical mode decomposition and wavelets for locating combined damage in a truss-type structure through vibration analysis. *Journal of Zhejiang University SCIENCE A, 14*, 615-630. doi:10.1631/jzus.A1300030

Joseph, L., & Larbi, N. (2001). Dynamic System Parameter Identification by Stochastic Realization Methods. *Journal of Vibration and Control - J VIB CONTROL, 7*, 711-728. doi:10.1177/107754630100700506

Le, T.-P., & Argoul, P. (2015). Distinction between harmonic and structural components in ambient excitation tests using the time–frequency domain decomposition technique. *Mechanical Systems and Signal Processing, 52-53*, 29-45. doi:https://doi.org/10.1016/j.ymssp.2014.07.008

Lim, H. C., & Ong, Z. C. (2016). *Development of adaptive phase control impact device for enhancement of frequency response function in operational modal testing*.

Lim, H. C., Ong, Z. C., & Brandt, A. (2018a). Implementation of phase controlled impact device for enhancement of frequency response function in operational modal testing. *Journal of the Franklin Institute, 355*(1), 291-313. doi:https://doi.org/10.1016/j.jfranklin.2017.11.031

Lim, H. C., Ong, Z. C., Ismail, Z., & Khoo, S. Y. (2018b). A performance study of controlled impact timing on harmonics reduction in operational modal testing. *Journal of Dynamic Systems, Measurement and Control, 141*(3), 034501-034056.

Maamar, A., Abdelghani, M., Le, T.-P., Gagnol, V., & Sabourin, L. (2019). Operational modal identification in the presence of harmonic excitation. *Applied Acoustics, 147*, 64-71. doi:https://doi.org/10.1016/j.apacoust.2018.02.017

Mohanty, P., & Rixen, D. J. (2004a). A modified Ibrahim time domain algorithm for operational modal analysis including harmonic excitation. *Journal of Sound and Vibration, 275*(1), 375-390. doi:https://doi.org/10.1016/j.jsv.2003.06.030

Mohanty, P., & Rixen, D. J. (2004b). Operational modal analysis in the presence of harmonic excitation. *Journal of Sound and Vibration, 270*(1), 93-109. doi:https://doi.org/10.1016/S0022-460X(03)00485-1

Universiti Malaya

Ong, Z. C., Kor, M. A. M. A., & Brandt, A. (2015). Experimental validation of phase synchronisation effects in optimising Impact-Synchronous Time Averaging. *6th International Operational Modal Analysis Conference, IOMAC 2015*.

Ong, Z. C., & Lee, C. C. (2015). Investigation of Impact Profile and Isolation Effect in Automated Impact Device Design and Control for Operational Modal Analysis. *Journal of Dynamic Systems, Measurement, and Control, 137*(9), 094504-094504-094505. doi:10.1115/1.4030526

Ong, Z. C., Lim, H. C., Khoo, S. Y., Ismail, Z., Kong, K. K., & Rahman, A. G. A. (2017). Assessment of the phase synchronization effect in modal testing during operation. *Journal of Zhejiang University-SCIENCE A, 18*(2), 92-105. doi:10.1631/jzus.A1600003

Ong, Z. C., Lim, H. C., Khoo, S. Y., Rahman, A. G. A., & Ismail, Z. (2016). An experimental investigation on the effects of exponential window and impact force level on harmonic reduction in impact-synchronous modal analysis. *Journal of Mechanical Science and Technology, 30*(8), 3523-3532. doi:10.1007/s12206-016-0712-6

Qi, K., He, Z., Li, Z., Zi, Y., & Chen, X. (2008). Vibration based operational modal analysis of rotor systems. *Measurement, 41*(7), 810-816. doi:https://doi.org/10.1016/j.measurement.2007.11.009

Rahman, A., Ismail, Z., Noroozi, S., & Chao, O. (2013). Impact-synchronous modal analysis (ISMA) - An attempt to find an alternative. *5th International Operational Modal Analysis Conference, IOMAC 2013*, 1-8.

Rahman, A., Ismail, Z., Noroozi, S., & Chao, O. (2014). Enhancement of Impact-synchronous Modal Analysis with number of averages. *Journal of Vibration and Control, 20*, 1645-1655. doi:10.1177/1077546312475147

Rahman, A. G. A., Ong, Z. C., & Ismail, Z. (2011a). Effectiveness of Impact-Synchronous Time Averaging in determination of dynamic characteristics of a rotor dynamic system. *Measurement, 44*(1), 34-45. doi:https://doi.org/10.1016/j.measurement.2010.09.005

Rahman, A. G. A., Ong, Z. C., & Ismail, Z. (2011b). Enhancement of coherence functions using time signals in Modal Analysis. *Measurement, 44*(10), 2112-2123. doi:https://doi.org/10.1016/j.measurement.2011.08.003

Thomson, W. T., & Dahleh, M. D. (2013). *Theory of Vibrations with Applications*: Pearson.

Xu, Y.-L., Zhang, X.-H., Zhu, S., & Zhan, S. (2016). Multi-type sensor placement and response reconstruction for structural health monitoring of long-span suspension bridges. *Science Bulletin, 61*(4), 313-329. doi:https://doi.org/10.1007/s11434-016-1000-7

Universiti Malaya